Maximizing Energy Efficiency in IRS-Assisted Phase Cooperative PS-SWIPT-Based Self-Sustainable IoT Network

HALEEMA SADIA [1], AHMAD KAMAL HASSAN [2], ZIAUL HAQ ABBAS [2], GHULAM ABBAS [3] (Senior Member, IEEE), THAR BAKER [4] (Senior Member, IEEE), AND NASIR SAEED [1] (Senior Member, IEEE)

[1]Department of Electrical and Communication Engineering, College of Engineering, United Arab Emirates University, Al Ain, UAE
[2]Faculty of Electrical Engineering, Ghulam Ishaq Khan Institute of Engineering and Technology, Topi 23460, Pakistan
[3]Faculty of Computer Science and Engineering, Ghulam Ishaq Khan Institute of Engineering and Technology, Topi 23460, Pakistan
[4]School of Architecture, Technology and Engineering, University of Brighton, BN2 4GJ Brighton, U.K.

CORRESPONDING AUTHOR: N. SAEED (e-mail: mr.nasir.saeed@ieee.org)

ABSTRACT Power splitting based simultaneous wireless information and power transfer (PS-SWIPT) appears to be a promising solution to support future self-sustainable Internet of Things (SS-IoT) networks. However, the performance of these networks is constrained by radio frequency signal strength and channel impairments. To overcome this challenge, intelligent reflecting surfaces (IRSs) have recently been introduced in IoT networks to improve network efficiency by controlling signal reflections. In this article, we propose a novel IRS-enabled phase cooperative framework that aims to maximize the energy efficiency (EE) of the PS-SWIPT based SS-IoT network. Our framework leverages the idea of phase cooperation between two distinct networks without requiring additional hardware resources. We employed transmit beamforming (BF) at access points (APs) and phase shift optimization at the IRS with effective phase cooperation between APs. The EE maximization problem turns out to be NP-hard, so first, an alternating optimization (AO) is solved for the user's network using heuristic BF approaches and phase optimization via semidefinite relaxation (SDR) approaches. To combat the computational complexity of AO, we also propose a low-complexity alternative solution by exploiting heuristic BF schemes and an iterative algorithm, i.e., the element-wise block-coordinate descent method for phase shifts optimization. The proposed solutions' analysis shows low computational complexity and fast convergence, achieving near-optimal EE performance for different network settings. We conducted extensive simulations to evaluate our proposed framework's performance and unveiled significant EE performance achieved by the IoT network consistent with the numerical findings. This work demonstrates the potential of IRS phase cooperation for enhancing the EE of different networks without constraining hardware resources.

INDEX TERMS Intelligent reflecting surface (IRS), SWIPT, power splitting, Internet of Things (IoT), beamforming, energy efficiency, phase cooperative network.

I. INTRODUCTION

WITH upsurge growth in wireless devices and user-diverse application needs, significant contributions are being made to investigate beyond fifth-generation (B5G) networks. A plethora of these networks are projected to meet the anticipated demands of improved spectral efficiency (SE) and energy efficiency (EE) by providing ubiquitous, reliable, and near-instant services with low power consumption [1], [2]. In transition to virtual reality, the next-generation Internet of Things (IoT) network appears as a paradigm shift and is envisioned to support a variety of wireless IoT devices (for example, smart phones, wearable devices, electronic tablets, smart security systems, sensors, etc.), paving the way for the future smart world [3]. Although these devices are equipped with diverse sensors, they are typically low-power and have limited battery life. Thus, these

devices need to be maintained regularly in order to extend the battery's lifespan [4]. These constraints limit the potential use of IoT networks due to higher costs, deployment challenges, and increased network complexity [5], [6].

Recently, radio frequency (RF) transmission-assisted simultaneous wireless information and power transfer (SWIPT) has received significant attention to address energy limitations and efficient information transfer for future self-sustainable (SS)-IoT networks [7], [8]. SWIPT offers low power, usually in μW, but provides wide coverage in a sustainable and controllable manner. By exploiting power splitting-based SWIPT (PS-SWIPT), the PS-based devices in SS-IoT networks first perform energy harvesting (EH) and then information decoding (ID) by employing wireless power transfer (WPT) and wireless information transfer (WIT) techniques simultaneously [9], [10], [11]. Apart from PS-SWIPT based SS-IoT networks, many investigations have considered separate network architectures where WPT and WIT techniques are employed by different energy harvesting receivers (EHRs) and information decoding receivers (IDRs), respectively [12]. PS-SWIPT based SS-IoT networks provide green communication with reduced capital expenditure as compared with separate network architectures [13]. However, due to different receiver sensitivities and application requirements in practical systems, these networks typically require significantly higher receive power in comparison to WIT networks [14]. Moreover, these networks are more susceptible to channel attenuation and are constrained by the received RF signal strength. Hence, in practical PS-SWIPT systems, poor efficiency of WPT for SS-IoT networks across large distances has been identified as the performance barrier. Although some studies have considered the massive multiple-input multiple-output (mMIMO) technique to enhance beamforming (BF) gain at the SWIPT transmitter to improve WPT efficiency, the main challenges for practical implementation remain high power consumption and hardware costs [15].

Intelligent reflecting surfaces (IRSs) have recently unlocked a novel communication paradigm to improve SE and EE for the sixth generation (6G) wireless networks [16], [17], [18]. It introduces the holographic idea of transmitting data by reusing an existing radio link, thus transforming the random wireless environment into a programmable one [19], [20]. The low-cost passive reflective elements of IRS can be reconfigured intelligently to modify the phase reflections of the incident signal. IRS passive nature results in significantly lower power consumption without introducing any thermal noise as compared to conventional relay-aided communication systems that rely on active transmission sources [21]. IRS can be easily deployed for both indoor and outdoor applications because of their low cost and compact size. With these alluring features, IRS is already being deployed in conventional wireless networks to improve key performance metrics through the optimization of adaptive parameters such as active and passive BF, IRS phase

shifts, transmission power, and effective IRS deployment [2], [22], [23], [24].

While the IRS serves to enhance conventional wireless communication networks performance, SWIPT applications are also attracted by the high BF gain achieved by passive IRS [12], [25], [26]. Many authors have considered IRS-supported WPT and WIT architectures with separate EHR and IDR to improve network performance. The authors in [27] investigated the optimization problem of weighted sum power maximization for EHRs. The authors demonstrated that the IRS-enabled SWIPT system did not require any specific energy-carrying signals and that sending information signals only to APs was adequate to service both IDR and EHR, independent of their channel realization. The authors in [28] solved the transmit power minimization problem in a multi-IRS framework by jointly optimizing transmit precoders and IRS phase shifts, subject to the quality-of-service (QoS) requirements of all receivers, i.e., the individual signal-to-interference-plus-noise ratio (SINR) constraints at IDR and EH constraints for EHR. The authors in [29] proposed a new dynamic IRS-BF scheme to improve the throughput of the IRS-enabled wireless communication framework. Joint optimization was performed to improve uplink and downlink wireless data transmission efficiency between hybrid access points and multiple wireless devices. To optimize the weighted sum rate (WSR) of all IDRs while adhering to the minimal EH criteria of all EHRs, the authors in [30] conducted a joint optimization. An optimal resource allocation algorithm for the IRS-supported SWIPT system was proposed by the authors in [12]. The authors minimized the transmission power on the AP subject to the QoS requirements of IDR and nonlinear EHR by joint optimization of BF and the transmission mode selection strategy. The authors in [31], [32] also exploited IRS to maximize the energy efficiency in secure SWIPT networks.

To unveil the potential advantages of SS-IoT networks, some investigations have also considered the IRS-supported SWIPT framework with integrated IDR/EHR. The authors performed WSR maximization in [13] for a dynamic SS-IoT network based on MIMO PS-SWIPT with IRS support. The authors solved the joint optimization problem with mutually exclusive constraints by providing an efficient optimization algorithm. The authors optimized the overall deployment of an IRS-powered wireless sensor network (WPSN) within [33] by combining the optimized IRS phase shifts and the transmission time allocation. By exploiting IRS assistance in the proposed framework, the efficiency of WPT and WIT techniques was enhanced. The authors in [34] maximized the EE of the IRS-enabled PS-SWIPT system by considering both the information signal and the dedicated energy signal at the AP. For maximizing system throughput of the wireless powered framework, the author in [35] provides a maximization solution by optimizing the IRS phase shifts, transmission time, and bandwidth. The authors of [36] investigated the same framework for multi-resource blocks with the objective of maximizing average throughput.

The aforementioned studies on IRS-enabled SWIPT-IoT networks primarily focus on optimizing various performance metrics by deploying IRS to serve IDRs and EHRs within either separated or integrated frameworks. These works commonly adopt separate designs for active beamforming/precoding vectors and passive phase shifts, and solve the corresponding optimization problems using joint or alternating optimization techniques. However, such approaches face several limitations, including the need for distinct phase shift configurations and additional IRS hardware to support multiple IDRs and EHRs across diverse network architectures. While the authors in [16], [22] introduced the concept of heterogeneous cognitive radio networks and employed IRS phase cooperation to enhance sum-rate performance, their analysis was restricted to user-centric networks. Moreover, the phase shift design in [22] did not account for inter-user interference, which may degrade overall network performance. To address these challenges and reduce system cost, this work proposes a novel IRS-enabled phase-cooperative framework for EE maximization in PS-SWIPT based SS-IoT networks. To the best of our knowledge, the exploitation of IRS phase cooperation in this specific context has not been explored in the existing literature.

A. MAIN CONTRIBUTIONS

To leverage the benefits of IRS in SWIPT networks, we propose a novel framework that utilizes IRS phase cooperation across two distinct networks, namely, the user network ($\mathtt{U}^{net}$) and the IoT network ($\mathtt{I}^{net}$). Both networks operate under the frequency division multiple access (FDMA) scheme to maximize the EE of a PS-SWIPT based SS-IoT network. Different from the existing works, our proposed framework focuses on the use of the IRS phase cooperation scheme in SWIPT IoT networks, which can significantly reduce hardware costs since no dedicated IRS deployment or separate phase shift design is required for the $\mathtt{I}^{net}$. The key contributions of this research are discussed next.

- This work presents an early attempt to solve the problem of EE maximization for an IRS-enabled PS-SWIPT based SS-IoT network using IRS phase cooperation method. The optimization problem is developed to provide improved EE of the proposed framework by exploiting the phase cooperation between $\mathtt{U}^{net}$ and $\mathtt{I}^{net}$ networks.

- For the proposed framework, the EE maximization problem is solved by optimizing the transmit BF vectors of $\mathtt{U}^{net}$ and $\mathtt{I}^{net}$, and IRS phase shifts of $\mathtt{U}^{net}$. The formulated optimization problem turns out to be NP-hard and arduous to solve directly. Therefore, we first provide an alternating optimization (AO) solution by employing active transmit BF optimization and passive phase shift optimization to solve the optimization problem at the $\mathtt{U}^{net}$. Transmit beamformers are optimized by closed-form sub-optimal heuristic BF solutions, namely, minimum-mean-square-error (MMSE)/regularized zero-forcing-BF (ZFBF) and ZFBF. Further, to solve for IRS

phase shifts optimization at the $\mathtt{U}^{net}$, a computationally efficient semidefinite relaxation (SDR) approach is employed. Moreover, the SDR relaxation's higher-rank solution is addressed by the Gaussian randomization method.

- Although the AO approach can solve the formulated problem efficiently, the SDR scheme results in significant computational complexity, particularly when a large number of IRS elements are used. To address this problem, we also propose an alternative low-complexity solution by leveraging the IRS's short-range/local coverage. This enables us to derive local optimal solutions to the phase shifts using a low-complexity iterative solution based on the element-wise block-coordinate descent (EBCD) method and BF vectors via a heuristic solution in closed form. The convergence analysis and computational complexity of the proposed solutions' unveil potential practical application implications.

- The performance gain in EE for the PS-SWIPT based SS-IoT network is assessed by optimizing the power splitting coefficient, transmit BF using a heuristic approach, and employing the $\mathtt{U}^{net}$ phase shifts via phase cooperation. Simulation results demonstrate that the EE of PS-SWIPT based SS-IoT networks can be significantly improved by employing IRS phase cooperation, which significantly reduces hardware installation cost without constraining resources at $\mathtt{U}^{net}$.

B. PAPER STRUCTURE AND NOTATIONS

We have organized this article into seven sections. Following an introduction in Section I, Section II, presents the proposed framework and related optimization problem formulations. Section III describes the AO technique for optimizing transmit beamformers and phase shifts. Section IV discusses the low-complexity alternative solution for the given problem. The EE optimization problem with the proposed solutions for IoT network is discussed in Section V of the paper. Simulation findings and related discussion is provided in Section VI. Section VII outlines our research conclusion and future directions.

Notations: In this work, scalar, vector, and matrix are represented by bold, lowercase, and uppercase letters, respectively. The complex matrix of the space $a \times b$ is denoted by the symbol $\mathbb{C}^{a \times b}$, and $\mathcal{CN}$ represents the complex Gaussian random variable. The absolute square, Euclidean norm, and Hermitian operator of a complex-valued vector $\mathbf{a}$ are denoted by $|a|^2$, $||\mathbf{A}||^2$, and $(\mathbf{a})^H$, respectively. The summation operator, the real part of a complex value, and the statistical expectation of random variables are represented by $\sum(\cdot)$, $\mathfrak{R}[\cdot]$, and $\mathbb{E}[\cdot]$, respectively.

II. SYSTEM MODEL AND PROBLEM FORMULATION
A. IRS-AIDED PHASE COOPERATIVE NETWORK

Figure. 1 shows an IRS-enabled downlink phase cooperative framework with a pair of $\mathtt{U}^{net}$ having K_I information decoding receivers/equipment's (R_k) and $\mathtt{I}^{net}$ having K_{E+I} EH

and information decoding devices (D_k). Both the networks are served through separate access points (A Ps), i.e., (AP_U) and (AP_I) for information transfer and energy+information transfer to U^{net} and I^{net}, respectively under multiple-input single-output (MISO) network configuration. The AP_U is fitted with M_U and AP_I with M_I transmit antennas such that $M_U \gg K_I$ and $M_I \gg K_{E+I}$, while each receiver pair has a single antenna. An FDMA protocol is predicated between APs for channel access, in which both U^{net} and I^{net} pairs operate on distinct license spectrum. Further, within each network, users access channels via a space-division multiple access (SDMA) scheme, where $K_{\{I,E+I\}}$ spatially separated receivers and devices are served simultaneously. An IRS with the N low-cost passive reflection elements equipped with a smart controller is installed between the AP_U and R_k. The AP_I shares the U^{net}'s IRS according to phase cooperation by exploiting the optimal phase shifts. The IRS controller maintains a separate wireless link with the APs to communicate channel state information (CSI), transmission data, and to receive IRS reflection coefficients designed at AP_U. Furthermore, for effective phase shifts cooperation, a dedicated link is used between AP_U and AP_I. Moreover, we assumed perfect CSI at the APs,[1] where information transfer between all nodes is solely performed at APs. The users are located in the vicinity of blocking objects; hence, they receive both IRS reflected (r) and direct (d) signals.

Now, consider that AP_U and AP_I broadcast K different messages spatially separated for transfer of information and energy signals to U^{net} and I^{net}, i.e., s_i $\{i \in K_I\}$ and s_j $\{j \in K_{E+I}\}$ with normalized power as $\mathbb{E}\{|s_i|^2\} = 1$ and $\mathbb{E}\{|s_j|^2\} = 1$. At U^{net} the signal received (y_{R_k}) by R_k with linear active transmit BF vector $\mathbf{w}_{R_k} \in \mathbb{C}^{M_U \times 1}$ at AP_U and passive phase shifts (Θ) at IRS after r multi-path reflections is given as in eq. (1)

$$y_{R_k} = \left(\mathbf{h}_{R_{r,k}}^H \Theta \mathbf{G}_R + \mathbf{g}_{R_{d,k}}^H\right) \sum_{i=1}^{K_I} \mathbf{w}_{R_i} s_i + z_{R_k}, \ \forall k \in K_I. \quad (1)$$

Next, AP_I uses U^{net}'s IRS phase shifts Θ, therefore at I^{net} the signal received by the D_k using AP_I active transmit BF vector $\mathbf{w}_{D_k} \in \mathbb{C}^{M_I \times 1}$ is given in eq. (2)

$$y_{D_k} = \left(\mathbf{h}_{D_{r,k}}^H \Theta \mathbf{G}_D + \mathbf{g}_{D_{d,k}}^H\right) \sum_{j=1}^{K_{E+I}} \mathbf{w}_{D_j} s_j$$
$$+ z_{D_k}, \ \forall k \in K_{E+I}, \quad (2)$$

where in (1) and (2), $\mathbf{h}_{R_{r,k}}^H \in \mathbb{C}^{1 \times N}$, $\mathbf{h}_{D_{r,k}}^H \in \mathbb{C}^{1 \times N}$ are the channel gains from the IRS to the U^{net} and I^{net}, respectively and $\mathbf{G}_R \in \mathbb{C}^{N \times M_U}$, $\mathbf{G}_D \in \mathbb{C}^{N \times M_I}$ show the respective channel gains from AP_U and AP_I to the IRS. The direct channel

[1]Although the CSI of IRS-enabled networks is often challenging to obtain, this work focuses on the upper bound for the system under investigation [36]. As a result, we presume perfect CSI for both APs and IRS [37], [38]. However, the accurate CSI can be obtained via multiple channel estimation algorithms investigated in the literature for IRS-enabled systems [39], [40], [41], [42]. Additionally, the proposed framework can be exploited further with an imperfect CSI scenario [43].
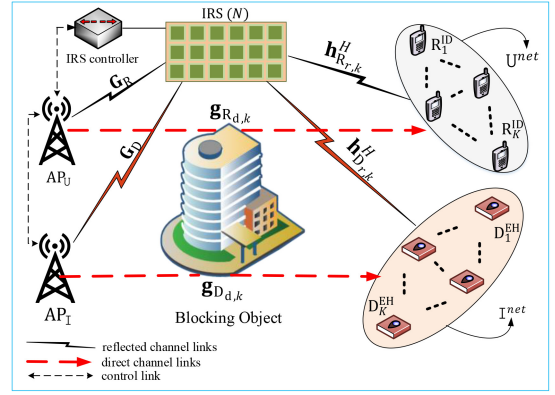

FIGURE 1. IRS-aided phase cooperative framework with users and PS-SWIPT based SS-IoT networks.

links from APs to users and IoT devices are represented by $\mathbf{g}_{R_{d,k}}^H$ and $\mathbf{g}_{D_{d,k}}^H$, respectively. The passive reflection matrix of U^{net}, represented by the diagonal matrix $\Theta \in \mathbb{C}^{N \times N}$, provides information on the amplitude and the phase shifts reflection coefficients, i.e.,

$$\Theta = \text{diag}\left(\beta_1 e^{j\theta_1}, \beta_2 e^{j\theta_2} \dots, \beta_N e^{j\theta_N}\right), \quad (3)$$

where $\beta_1, \dots, \beta_N \in [0, 1]$ and $\theta_1, \dots, \theta_N \in [0, 2\pi)$ show the fixed amplitude reflection coefficients and IRS phase shifts variables, respectively. In literature, the amplitude reflection model is frequently assumed fixed, i.e., $\beta_n = 1, \forall n \in N$ to eliminate hardware complexity overhead [20]. The factors $z_{R_k} \in \mathcal{CN}(0, \sigma_k^2)$, and $z_{D_k} \in \mathcal{CN}(0, \sigma_k^2)$ denote the respective receiver additive noise with variance σ_k^2 at R_k and D_k.

At U^{net}, the SINR (Γ_{R_k}) expression for the kth receiver is given by eq. (4)

$$\Gamma_{R_k} = \frac{\left|\left(\mathbf{h}_{R_{r,k}}^H \Theta \mathbf{G}_R + \mathbf{g}_{R_{d,k}}^H\right)\mathbf{w}_{R_k}\right|^2}{\sum_{i \neq k} \left|\left(\mathbf{h}_{R_{r,k}}^H \Theta \mathbf{G}_R + \mathbf{g}_{R_{d,k}}^H\right)\mathbf{w}_{R_i}\right|^2 + \sigma_k^2}, \ \forall k \in K_I,$$
$$(4)$$

where $\sum_{i \neq k} |(\mathbf{h}_{R_{r,k}}^H \Theta \mathbf{G}_R + \mathbf{g}_{R_{d,k}}^H)\mathbf{w}_{R_i}|^2$ is representing interference term encountered by kth receiver.

The achievable rate of R_k can be denoted in eq. (5) by

$$\mathcal{R}_{R_k} = \log_2\left(1 + \Gamma_{R_k}\right), \ \forall k \in K_I. \quad (5)$$

Accordingly, the sum rate ($\mathcal{R}_k$) of U^{net} is calculated as

$$\mathcal{R}_k^{U^{net}} = \sum_{k=1}^{K_I} \mathcal{R}_{R_k}, \ \forall k \in K_I. \quad (6)$$

B. PS-SWIPT IMPLEMENTATION AT SS-IOT NETWORK
In order to decode information signals, the SS-IoT devices require adequate energy, which is usually not available because of the low energy resources of the IoT network. Therefore, the received signal power is split for EH and ID by PS-based SS-IoT devices [44], [45]. Power splitting enables the simultaneous implementation of EH and ID [46], in contrast to time switching, which mandates distinct time

slots for both processes [47]. In order to efficiently decode their data, the devices used part of the received signal power for EH and the remaining part for ID. We assume that the received signal power is divided into (φ_k) and $(1 - \varphi_k)$ as the power harvesting coefficient and the ID coefficient by D_{K_I} devices, respectively. Furthermore, as we are employing a power splitting scheme, we consider that the entire transmission is taking place in a single time slot, T.

IoT devices receive a fraction of the power from y_{D_k}, that is, φ_k for EH and the remaining fraction $(1 - \varphi_k)$ for decoding information. After performing EH, the received signal available for ID is represented as in eq. (7)

$$
\begin{aligned}
y_{D_k}^{ID} &= \sqrt{1 - \varphi_k} y_{D_k} + \omega_{e\,h} \\
&= \sqrt{1 - \varphi_k} \Big(\mathbf{h}_{D_{r,k}}^H \Theta \mathbf{G}_D + \mathbf{g}_{D_{d,k}}^H \Big) \sum_{j=1}^{K_{E+I}} \mathbf{w}_{D_j} s_j \\
&\quad + \sqrt{1 - \varphi_k} z_{D_k} + \omega_{e\,h}, \ \ \forall k \in K_{E+I},
\end{aligned} \tag{7}
$$

here, $\omega_{e\,h}$ is representing the thermal noise introduced by the circuitry due to phase offset (with zero mean and σ^2 variance) [48]. Furthermore, the noise factor after EH, i.e., $(\sqrt{1 - \varphi_k}) z_{D_k}$, is very small and can be ignored. Consequently, the information signal received at the kth SS-IoT device (D_k) after EH is represented as in eq. (8)

$$
\begin{aligned}
y_{D_k}^{ID} &= \Big(\sqrt{1 - \varphi_k} \Big) \Big(\mathbf{h}_{D_{r,k}}^H \Theta \mathbf{G}_D + \mathbf{g}_{D_{d,k}}^H \Big) \sum_{j=1}^{K_{E+I}} \mathbf{w}_{D_j} s_j \\
&\quad + \omega_{e\,h}, \ \ \forall k,
\end{aligned} \tag{8}
$$

The corresponding SINR expression is given by

$$
\Gamma_{D_k}^{ID} = \frac{(1 - \varphi_k) |\big(\mathbf{h}_{D_{r,k}}^H \Theta \mathbf{G}_D + \mathbf{g}_{D\,d,k}^H \big) \mathbf{w}_{D_k}|^2}{\sum_{j \neq k} (1 - \varphi_k) |\big(\mathbf{h}_{D_{r,k}}^H \Theta \mathbf{G}_D + \mathbf{g}_{D\,d,k}^H \big) \mathbf{w}_{D_j}|^2 + \sigma_k^2}, \ \forall k, \tag{9}
$$

where $\sum_{j \neq k} (1 - \varphi_k) |(\mathbf{h}_{D_{r,k}}^H \Theta \mathbf{G}_D + \mathbf{g}_{D\,d,k}^H) \mathbf{w}_{D_j}|^2$ denotes the interference term encountered by the kth device of $\mathtt{I}^{net}$. Consequently, the achievable rate of R_k and the sum rate of $\mathtt{I}^{net}$ can be stated in eq. (10) and eq. (11), respectively as

$$
\mathcal{R}_{D_k} = \log_2 \big(1 + \Gamma_{D_k}^{ID} \big), \ \ \forall k \in K_{E+I}. \tag{10}
$$

$$
\mathcal{R}_k^{\mathtt{I}^{net}} = \sum_{k=1}^{K_{E+I}} \mathcal{R}_{D_k}, \ \ \forall k \in K_{E+I}. \tag{11}
$$

Similarly, the received signal for EH is given by

$$
\begin{aligned}
y_{D_k}^{EH} &= \sqrt{\varphi_k} y_{D_k} \\
&= \sqrt{\varphi_k} \Big(\mathbf{h}_{D_{r,k}}^H \Theta \mathbf{G}_D + \mathbf{g}_{D_{d,k}}^H \Big) \sum_{j=1}^{K_{E+I}} \mathbf{w}_{D_j} s_j + \sqrt{\varphi_k} z_{D_k}, \\
&\qquad \forall k.
\end{aligned} \tag{12}
$$

Here, the power harvested from additive noise, i.e., $\sqrt{\varphi_k} z_{D_k}$, is very low compared with signal harvesting power and hence can be neglected [34], [49]. The D_k can only decode their

data when they have a sufficient amount of energy. Therefore, the amount of energy harvested by D_k is provided by eq. (13)

$$
E_{\mathcal{H}_k} = \varphi_k \sum_{k=1}^{K_{E+I}} |\big(\mathbf{h}_{D_{r,k}}^H \Theta \mathbf{G}_D + \mathbf{g}_{D_{d,k}}^H \big) \mathbf{w}_{D_k}|^2 \mu_k, \ \ \forall k \in K_{E+I},
$$

$$
\tag{13}
$$

where $\mu_k \in [0, 1]$ represents the circuitry's EH efficiency. The PS-SWIPT technique is utilized effectively at $\mathtt{I}^{net}$, which results in effective communication by exploiting passive IRS phase shifts at $\mathtt{U}^{net}$ and active BF at $AP_{\mathtt{I}}$.

C. FORMULATION OF OPTIMIZATION PROBLEM

For the proposed IRS-enabled phase cooperative network (PC$_{Net}$), our objective is to maximize the EE of $\mathtt{I}^{net}$. Therefore, to perform EE maximization, we first optimize the power harvesting coefficient, which improves $\mathtt{I}^{net}$ EH power. Next, we optimize the precoding vectors $\mathbf{w}_{D_k}$ of $AP_{\mathtt{I}}$ by exploiting the optimal phase shifts of $\mathtt{U}^{net}$ while keeping the transmit power of $AP_{\mathtt{I}}$ to a minimum. Compared to joint optimization techniques, this sequential approach significantly reduces complexity and hardware cost, while it can partially compromise the whole cooperative potential. For solving optimization problems, we initially calculate the total power consumption in the proposed framework, which depends on multiple parameters. Therefore, for $\mathtt{I}^{net}$, let us define $\eta \in [0, 1]$ as the power amplifier efficiency at $AP_{\mathtt{I}}$, hence the total circuit power (P_C) consumed at $AP_{\mathtt{I}}$ is denoted by $P_C = \eta + P_{AP_{\mathtt{I}}} + \sum_{k=1}^{K_{E+I}} P_{D_k}$, where $P_{AP_{\mathtt{I}}}$ denotes the overall static power consumption at the $AP_{\mathtt{I}}$. At the kth IoT device terminal, P_{D_k} indicates the hardware power dissipation. By assuming perfect CSI at all nodes, we perform EE maximization of $\mathtt{I}^{net}$ by optimization of the PS coefficient; φ_k $\{\forall k \in K_{E+I}\}$, transmit BF vectors; $\mathbf{W}_{\mathtt{I}}$ $\{\mathbf{W}_{\mathtt{I}} = [\mathbf{w}_1, \ldots, \mathbf{w}_{K_{E+I}}] \in \mathbb{C}^{M_{\mathtt{I}} \times K_{E+I}}\}$, and employing optimized phase shifts of $\mathtt{U}^{net}$ with minimum transmit power constraint.

Taking into consideration PS coefficients, individual data rate limitations of the devices, and the total transmit power budget, EE is obtained by dividing the sum rate of the devices by the total power consumption of the network. The EE optimization problem for $\mathtt{I}^{net}$ is represented as follows:

$$
(P_1): \max_{\varphi, \mathbf{W}_{\mathtt{I}}, \Theta} \ \frac{\mathcal{R}_k^{\mathtt{I}^{net}}}{1/\eta \sum_{k=1}^{K_{E+I}} ||\mathbf{w}_{D_k}||^2 + P_C} \tag{14a}
$$

$$
\text{s. t.} \ \ \Gamma_{D_k}^{ID} \geq \Gamma_{D_{k,\min}}, \ \ \forall k \in K_{E+I}, \tag{14b}
$$

$$
\sum_{k=1}^{K_{E+I}} ||\mathbf{w}_{D_k}||^2 \leq P_{AP_{\mathtt{I}}}, \tag{14c}
$$

$$
f(\mathcal{E}) \ \geq \frac{\bar{E}_{\mathcal{H}_k}}{\varphi_k \mu_k}, \ \ \forall k \in K_{E+I}, \tag{14d}
$$

$$
|\Theta_{k,n,n}| = 1, \ \ \forall n \in N, \tag{14e}
$$

$$
0 \leq \theta_{k,n} \leq 2\pi, \ \ \forall n \in N, \tag{14f}
$$

$$
0 < \varphi_k < 1, \ \ \forall k \in K_{E+I}, \tag{14g}
$$

TABLE 1. Qualitative comparison of proposed single IRS framework with multi-IRS frameworks.

Feature	Single IRS (Phase Cooperation)	Multi-IRS Networks
Hardware Constrains	Lower cost	Higher cost
Power Consumption	Lower	Higher
Network Management	Simplified	Complex
Deployment Cost	Lower	Higher
Optimization Complexity	Lower	Higher

where optimization variables are implicitly considered in the objective function for notational brevity, and $f(\mathcal{E}) = \sum_{k=1}^{K_{E+I}} |(\mathbf{h}_{D_r,k}^H \Theta \mathbf{G}_D + \mathbf{g}_{D_d,k}^H) \mathbf{w}_{D_k}|^2$ is used for notational simplicity. The constraint (14b) ensures the QoS requirements, with $\Gamma_{D_{k,\min}} = 2^{\mathcal{R}_{D_{k,\min}}} - 1$, showing the minimum SINR requirement of the k-th IoT device for ID, and $\mathcal{R}_{D_{k,\min}}$ represents the minimum data rate required. The maximum transmission power P_{AP_I} at AP_I is constrained by (14c), where $||\mathbf{w}_{D_k}||^2$ and θ_n illustrate the respective Euclidean-norm of $\mathbf{w}_{D_k}$ and the n-th element of Θ. The constraint (14d) guarantees the EH requirements of the devices employing $\bar{E}_{\mathcal{H}_k}$ as the minimum amount of energy harvested. The constraints (14e) and (14f), respectively, define the passive nature of the reflecting elements of the IRS and the phase shifts range, while the constraint (14g) represents the bound range of PS coefficients.

Because of the non-convex objective function and coupled optimization variables, it appears clearly that (P$_1$) cannot be solved directly. Furthermore, (14d) and (14f) have PS relationship constraints that further complicate (P$_1$) because the feasible region of the PS ratio is not always non-empty. Therefore, to solve (P$_1$), an alternating optimization solution is proposed for the given framework by dividing the original optimization problem into sub-problems and solving them by employing effective phase cooperation between networks. To exploit the optimal phase shifts, we solve the problem by first optimizing passive phase shifts of U^{net} using AO and then using those optimized fixed phase shifts Θ to maximize EE at I^{net} using EH coefficients and active BF optimization.

III. ALTERNATING OPTIMIZATION SOLUTION FOR U^{NET}
To solve (P$_1$), an optimization problem is first formulated for U^{net} to obtain the optimal phase shifts. Hence, an EE maximization problem similar to (P$_1$) is developed for the U^{net}, and a solution is provided via an AO. In particular, we dissociate problem (P$_1$) into passive phase shifts optimization and active BF optimization sub-problems for U^{net} and address them alternatively. To solve (P$_1$) via AO, we employed low computational heuristic sub-optimal solutions, i.e., MMSE and ZFBF, to obtain the beamformers; $\mathbf{W}_U \{\mathbf{W}_U = [\mathbf{w}_1, \ldots, \mathbf{w}_{K_I}] \in \mathbb{C}^{M_U \times K_I}\}$ with closed-form solutions, while the passive phase shifts of U^{net} are optimized using a semi-definite programming (SDP) approach. Further, it is noticeable that IRS is deployed for U^{net}; therefore, in the case of IRS-enabled U^{net}, the total power consumed is given by $P_C = \eta + P_{AP_U} + P_N + \sum_{k=1}^{K_I} P_{R_k}$, where the

factor P_N denotes the power consumption at the IRS terminal and P_{R_k} shows power dissipation at the k-th user device. Hence, similar to (P$_1$) but only with the WIT technique, the optimization problem for U^{net} with only ID receivers is formulated as

$$(P_2): \max_{\mathbf{W}_U, \Theta} \quad \frac{\mathcal{R}_k^{U^{net}}}{1/\eta \sum_{k=1}^{K_I} ||\mathbf{w}_{R_k}||^2 + P_C} \quad (15a)$$

$$\text{s. t.} \quad \Gamma_{R_k} \geq \Gamma_{R_{k,\min}}, \quad \forall k \in K_I, \quad (15b)$$

$$\sum_{k=1}^{K_I} ||\mathbf{w}_{R_k}||^2 \leq P_{AP_U}, \quad (15c)$$

$$|\Theta_{k,n,n}| = 1, \quad \forall n \in N, \quad (15d)$$

$$0 \leq \theta_{k,n} \leq 2\pi, \quad \forall n \in N, \quad (15e)$$

here, $\Gamma_{R_{k,\min}} = 2^{\mathcal{R}_{R_{k,\min}}} - 1$ presents the k-th IDR minimum SINR requirement, and $\mathcal{R}_{R_{k,\min}}$ shows the minimum data rate required by R_k receiver. The factors $||\mathbf{w}_{R_k}||^2$ represent the Euclidean-norm of $\mathbf{w}_{R_k}$ and θ_n signify the n-th element of Θ. The maximum transmission power available at AP_U is denoted by P_{AP_U}. While (P 2) bears structural resemblance to prior works [2], [30], [31], its exploration within the novel framework of phase cooperation remains unaddressed in existing literature. It is also notable that many authors solved the optimization objectives for multi-IRS frameworks [27], [28]. Although considering multi-IRS can improve signal reflections and coverage, it also increases hardware costs and complexity compared with the single-IRS scenarios. Furthermore, the optimization problem gets more simplified by employing phase cooperation compared to multi-IRS scenarios. A qualitative comparison between single and multi-IRS frameworks is also provided in Table 1. Hence, unlike these earlier studies, our formulation uniquely incorporates phase alignment across distributed elements, introducing a new dimension to the optimization problem. Furthermore, (P$_2$) poses significant computational challenges due to the non-convex nature of the objective function and the related constraints outlined in (15b), (15c), and (15e), which have not been tackled in this specific context before. Therefore, to solve (P$_2$), we perform AO by first exploiting linear BF optimization for the given phase shifts, and then phase optimization is performed for the obtained sub-optimal beamformers.

A. TRANSMIT BEAMFORMING OPTIMIZATION
(P$_2$) is transformed into an EE maximization problem under the individual user's data rate constraint for a given Θ. Hence, for U^{net} the (P$_2$) is reformulated into sub-problem as follows

$$(P_{2.1}): \max_{\mathbf{W}_U} \quad \frac{\mathcal{R}_k^{U^{net}}}{1/\eta \sum_{k=1}^{K_I} ||\mathbf{w}_{R_k}||^2 + P_C} \quad (16a)$$

$$\text{s. t.} \quad (15b), (15c) \quad (16b)$$

The stated constraints allow (P$_{2.1}$) to be tractable; as a result, the heuristic closed-form BF schemes are investigated below to obtain sub-optimal solution.[2]

Heuristic Approach: The SE and EE of B5G wireless communication networks are significantly enhanced by adaptive transmit BF [50]. In literature, a multitude of exhaustive and heuristic BF schemes are investigated to provide optimal and sub-optimal solutions for different network architectures [51]. Therefore, to avoid the computational complexity of optimal transmit BF schemes, in this article we employ two heuristic BF approaches, i.e., transmit MMSE/regularized ZFBF and ZFBF, as our proposed framework is designed to facilitate low power SWIPT IoT applications and provide solution for the NP-hard multiuser transmit BF problem. Albeit these schemes provide sub-optimal solutions, they are the least complex, provide closed-form solutions, and can be easily tweaked to provide the nearest optimal solution under special cases.

Although (P$_{2.1}$) is tractable, if the users required data rate increases or the AP$_U$ transmit power lowers, the maximization problem becomes infeasible for a given Θ under the constraint (15b). To solve this, (P$_{2.1}$) is reformulated as a power minimization problem given as

$$\left(P_{2.1}^*\right) : \min_{\mathbf{W}_U} \sum_{k=1}^{K_I} ||\mathbf{w}_{R_k}||^2 \tag{17a}$$

$$\text{s.t. } \Gamma_{R_k} \geq \Gamma_{R_{k,\min}}, \ \forall k \in K_I. \tag{17b}$$

(P$_{2.1}^*$) clearly contains a convex objective function and can be traced using different convex approximation techniques, including second-order cone program (SOCP) [52], [53], semidefinite programming (SDP) [54], [55] under the minimum transmit power, or a fixed-point iteration algorithm [56], [57]. However, to solve the hidden convexity of constraint (15b), we employed the inner product property of phase rotation from [50], which states that for absolute values of SINRs, the inner product of signal power is positive and real valued, i.e., $\sqrt{|(\mathbf{h}_{R_{r,k}}^H \Theta \mathbf{G}_R + \mathbf{g}_{R_{d,k}}^H)\mathbf{w}_{R_k}|^2} = (\mathbf{h}_{R_{r,k}}^H \Theta \mathbf{G}_R + \mathbf{g}_{R_{d,k}}^H)\mathbf{w}_{R_k} \geq 0$. Additionally, let's define twofold channel gains as follows for ease of representation: $\mathbf{f}_{R_k}^H = (\mathbf{h}_{R_{r,k}}^H \Theta \mathbf{G}_R + \mathbf{g}_{R_{d,k}}^H)$. Hence, using the inner product property, the constraint (15b) can be reformulated as [58]

$$\frac{1}{\Gamma_{R_{k,\min}} \sigma_k^2} |\mathbf{f}_{R_k}^H \mathbf{w}_{R_k}|^2 \geq \sum_{i \neq k} \frac{1}{\sigma_k^2} |\mathbf{f}_{R_k}^H \mathbf{w}_{R_k}|^2 + 1 \Leftrightarrow$$

$$\frac{1}{\sqrt{\Gamma_{R_{k,\min}} \sigma_k^2}} \mathbb{R}\left(\mathbf{f}_{R_k}^H \mathbf{w}_{R_k}\right) \geq \sqrt{\sum_{i \neq k} \frac{1}{\sigma_k^2} |\mathbf{f}_{R_k}^H \mathbf{w}_{R_k}|^2 + 1}, \tag{18}$$

here, $\mathbb{R}\{\cdot\}$ shows the real part; so, (18) provides a reformulated SINR that is a convex second-order cone constraint [50], [59]. Now, by using this new constraint (18), (P$_{2.1}^*$) can be solved feasibly using convex optimization

[2]Heuristic BF schemes discussed in Section III are applied to both U^{net} and I^{net}. Here, general notations are used, i.e., $k \in K_{\{I,E+I\}}$.

theory [50], [58]. Specifically, the strong duality and Karush Kuhn Tucker (KKT) conditions are sufficient to solve (P$_{2.1}^*$) [60]. Hence, by employing strong duality and KKT conditions, the Lagrangian function defined for (P$_{2.1}^*$) is obtained as

$$\mathcal{L}(\mathbf{W}_I, \Lambda_I) = \sum_{k=1}^{K_I} ||\mathbf{w}_{R_k}||^2 + \sum_{k=1}^{K_I} \lambda_k \Big(\sum_{i \neq k} \frac{1}{\sigma_k^2} |\mathbf{f}_{R_k}^H \mathbf{w}_{R_i}|^2 + 1$$
$$- \frac{1}{\Gamma_{R_{k,\min}} \sigma_k^2} |\mathbf{f}_{R_k}^H \mathbf{w}_{R_k}|^2 \Big), \tag{19}$$

where $\Lambda_I = [\lambda_1, \ldots, \lambda_{K_I}]$, $\lambda_k \geq 0$ ($k \in \{1, \ldots, K_I\}$) is the Lagrangian multiplier associated with the k-th SINR constraint and can be computed using convex optimization or fixed point equations [61]. The dual function is $\min_{\mathbf{w}_1, \mathbf{w}_2, \ldots, \mathbf{w}_{K_I}} \mathcal{L} = \sum_{k=1}^{K_I} \lambda_k$ and the strong duality property of [(P$_{2.2}$), [62]] implies that the total power is $\sum_{k=1}^{K_I} ||\mathbf{w}_{R_k}||^2$. By exploiting KKT conditions from [60] and using a power allocation scheme discussed in [58] (Theorem 3.16), the optimal BF vector for (P$_{2.1}^*$) under given Θ is expressed as

$$\mathbf{w}_{R_k}^* = \sqrt{P_k} \bar{\mathbf{w}}_{R_k}^*, \quad \text{where} \quad \bar{\mathbf{w}}_{R_k}^*$$
$$= \frac{\left(\mathbf{I}_{M_U} + \sum_{i=1}^{K_I} \frac{\lambda_i}{\sigma_k^2} \mathbf{f}_{R_i} \mathbf{f}_{R_i}^H\right)^{-1} \mathbf{f}_{R_k}}{\left\|\left(\mathbf{I}_{M_U} + \sum_{i=1}^{K_I} \frac{\lambda_i}{\sigma_k^2} \mathbf{f}_{R_i} \mathbf{f}_{R_i}^H\right)^{-1} \mathbf{f}_{R_k}\right\|}, \tag{20}$$

where the factor P_k shows the BF power at the AP$_U$ and $\bar{\mathbf{w}}_{R_k}^*$ signify the uniform BF direction for k-th user. The factor $\mathbf{I}_{M_U}$ shows the identity matrix. Since we obtain the BF directions, the unknown power factors associated with K_I users can be obtained by using the equality condition of constraint (18) at the optimal solution. Hence, for K_I known BF linear equations, the corresponding power factors can be obtained as [62]

$$\begin{bmatrix} P_1 \\ \vdots \\ P_{K_I} \end{bmatrix} = \mathbf{A}^{-1} \begin{bmatrix} \sigma_1 \\ \vdots \\ \sigma_{K_I} \end{bmatrix}, \tag{21}$$

$$\text{where } [\mathbf{A}]_{ij} = \begin{cases} \frac{1}{\Gamma_{R_{k,\min}}} |\mathbf{f}_{R_k}^H \bar{\mathbf{w}}_{R_k}|^2, & i = j, \\ -|\mathbf{f}_{R_k}^H \bar{\mathbf{w}}_{R_k}|^2, & i \neq j, \end{cases}.$$

Now, (20) and (21) combined provide an optimal closed-form BF solution for (P$_{2.1}^*$) as a function of simple Lagrange multipliers. Using this optimal BF structure obtained by solving (P$_{2.1}^*$), we can easily solve our original EE optimization problem, i.e., (P$_{2.1}$). The solution to (P$_{2.1}^*$), provides optimal BF vectors under minimum transmit power; therefore, this solution can feasibly satisfy the constraint (15b) of (P$_{2.1}$). Further, using optimal BF vectors of (P$_{2.1}^*$), the optimal BF solution for (P$_{2.1}$) is provided as

$$\mathbf{w}_{R_k}^* = \sqrt{P_k} \frac{\left(\mathbf{I}_{M_U} + \sum_{i=1}^{K_I} \frac{\lambda_i}{\sigma_k^2} \mathbf{f}_{R_i} \mathbf{f}_{R_i}^H\right)^{-1} \mathbf{f}_{R_k}}{\left\|\left(\mathbf{I}_{M_U} + \sum_{i=1}^{K_I} \frac{\lambda_i}{\sigma_k^2} \mathbf{f}_{R_i} \mathbf{f}_{R_i}^H\right)^{-1} \mathbf{f}_{R_k}\right\|}, \ \forall k \in K_I. \tag{22}$$

For K_I users, the matrix inversion in (22) remains the same; hence the optimal BF matrix for $\mathtt{I}^{net}$ can be represented as $\mathbf{W}_U^*$ $\{\mathbf{W}_U^* = [\mathbf{w}_1^*, \ldots, \mathbf{w}_{K_I}^*] \in \mathbb{C}^{M_U \times K_I}\}$ and the channel matrix for IRS-enabled network as $\mathbf{F}_U = [\mathbf{f}_1, \mathbf{f}_2, \ldots, \mathbf{f}_K] \in \mathbb{C}^{M_U \times K_I}$ where $\mathbf{f}_{R_k}^H = (\mathbf{h}_{R_{r,k}}^H \Theta \mathbf{G}_R + \mathbf{g}_{R_{d,k}}^H)$. The resultant combined channel response can be expressed as $\sum_{i=1}^{K_I} \frac{\lambda_i}{\sigma_k^2} \mathbf{f}_{R_i} \mathbf{f}_{R_i}^H = \frac{1}{\sigma^2} \mathbf{F}_U \Lambda \mathbf{F}_U^H$. Thus, it is feasible to derive the compact BF matrix as

$$\mathbf{W}_U^* = \left(\mathbf{I}_{M_U} + \frac{1}{\sigma^2} \mathbf{F}_U \Lambda \mathbf{F}_U^H\right)^{-1} \mathbf{F}_U \mathbf{P}^{\frac{1}{2}}, \tag{23}$$

where $\Lambda = \text{diag}(\lambda_1, \ldots, \lambda_{K_I})$, is a diagonal matrix having K_I λ-parameters. $\mathbf{P}^{\frac{1}{2}}$ shows the square root of power allocation matrix given as $\mathbf{P} = \text{diag}(P_1/||(\mathbf{I}_{M_U} + \frac{1}{\sigma^2} \mathbf{F}_U \Lambda \mathbf{F}_U^H)^{-1} \mathbf{f}_1||^2, \ldots, P_{K_I}/||(\mathbf{I}_{M_U} + \frac{1}{\sigma^2} \mathbf{F}_U \Lambda \mathbf{F}_U^H)^{-1} \mathbf{f}_{K_I}||^2)$. So, the optimum BF from (23) will provide the optimal SINR, which in result maximizes $(P_{2.1})$.

The closed-form BF solutions for the ZFBF and transmit MMSE/Regularized ZFBF schemes are presented below using (23).

1) ZFBF

ZFBF is a potential technique for reducing inter-user interference [63], [64]. It is referred to as the channel inversion scheme since it contains the channel matrix's pseudo-inverse $\mathbf{F}_U^H$, i.e., $\mathbf{F}_U(\mathbf{F}_U^H \mathbf{F}_U)^{-1}$. When using ZFBF, interference power is reduced while SINR is optimized. By cancelling noise and interference, this criteria decouples the selection of the BF direction. Hence, using asymptotic properties from [58], the relation for ZFBF is obtained as

$$\mathbf{W}_U^{*(ZFBF)} = \mathbf{F}_U\left(\mathbf{F}_U^H \mathbf{F}_U\right)^{-1} \Lambda^{-1} \bar{\mathbf{P}}, \tag{24}$$

where the factor $\bar{\mathbf{P}}$ shows the modified power allocation matrix provided as $\bar{\mathbf{P}} = \text{diag}(P_1/||(\sigma^2 \mathbf{I}_{K_I} + \Lambda \mathbf{F}_U^H \mathbf{F}_U)^{-1} \mathbf{f}_1||^2, \ldots, P_{K_I}/||(\sigma^2 \mathbf{I}_{K_I} + \Lambda \mathbf{F}_U^H \mathbf{F}_U)^{-1} \mathbf{f}_{K_I}||^2)$. At large SNRs, ZFBF is considered to be the asymptotic optimal option; nevertheless, performance degrades at moderate SNRs.

2) TRANSMIT MMSE/REGULARIZED ZFBF

In a multi-user scenario, MMSE is acclaimed as the sub-optimal heuristic solution because it can overcome ZFBF's asymptotic optimality and provide better results at intermediate SINRs. Hence, using (20) and (21) and setting $\lambda_k = \lambda$, $\forall k \in K_I$, the subsequent expression for MMSE optimal BF is obtained as

$$\mathbf{W}_U^{*(MMSE)} = \mathbf{F}_U\left(\mathbf{I}_{K_I} + \frac{\lambda}{\sigma^2} \mathbf{F}_U^H \mathbf{F}_U\right)^{-1} \mathbf{P}^{\frac{1}{2}}. \tag{25}$$

Expression (25) is also named as regularized ZFBF [64], [65] as it contains an identity matrix, which acts as a regularization matrix in (25). Here, λ is referred as the regularization parameter that satisfies the sum property of transmission power, i.e., $\sum_{i=1}^{K_I} \lambda_i = P$ with $\lambda = P/K$. Consequently, using a standard line search method, (25) provides an optimal

solution for a particular transmission case by adjusting the λ-parameter.

B. PASSIVE PHASE OPTIMIZATION

By utilizing the optimal transmit beamformers $\mathbf{W}_U^*$ obtained in Section III-A, the phase shifts optimization can be solved for (P_2). The reformulated sub-problem is given as

$$(P_{2.2}) : \max_{\Theta} \frac{\mathcal{R}_k^{v^{net}}}{1/\eta \sum_{k=1}^{K_I} ||\mathbf{w}_{R_k}||^2 + P_C} \tag{26a}$$

$$\text{s.t. } (15b), \ (15d), \ (15e) \tag{26b}$$

The non-convex constraints make $(P_{2.2})$ an NP-hard optimization problem; however, by making a few variable changes, the problem can be feasibly transformed into a tractable form. Let $\mathbf{h}_{R_{r,k}}^H \Theta \mathbf{G}_R \mathbf{w}_{R_k}^* = \boldsymbol{v}^H \mathbf{a}_{i,k}$ and $\mathbf{h}_{D_{d,k}}^H \mathbf{w}_{R_k}^* = b_{i,k}$ where $\boldsymbol{v} = [v_1, \ldots, v_N]^H$ for $v_n = e^{j\theta_n}, \forall n \in N$ and $\mathbf{a}_{i,k} = (\mathbf{h}_{R_{r,k}}^H) \Theta \mathbf{G}_R \mathbf{w}_{R_k}^* \in \mathbb{C}^{N_{IRS} \times 1}$. Also, it is notable that although the same IRS phase shifts matrix, Θ, is shared by all the users, the SINR constraints in (15b) are not always mandated to be satisfied for a feasible solution of $(P_{2.2})$. As a result, a slack variable, β_k, is introduced to deal with the K_I residual SINR. The reformulated sub-problem is stated as follows by substituting new variables

$$\left(P_{2.2}^*\right) : \max_{\boldsymbol{v}, \{\beta_k\}_{k=1}^{K_I}} \quad \sum_{k \in K_I} \beta_k \tag{27a}$$

$$\text{s.t. } \frac{|\boldsymbol{v}^H \mathbf{a}_{k,k} + b_{k,k}|^2}{\sum_{i \neq k}^{K_I} |\boldsymbol{v}^H \mathbf{a}_{i,k} + b_{i,k}|^2 + \sigma_k^2} \geq \Gamma_{R_{k,\min}} + \beta_k, \tag{27b}$$

$$|v_n| = 1, \quad \forall n \in N, \quad \beta_k \geq 0, \quad \forall k \in K_I. \tag{27c}$$

where (15d) transforms into a non-convex unit-modulus constraint, i.e., $|v_n|^2 = 1, \forall n$. Although $(P_{2.2^*})$ is a non-convex optimization problem, the fully separable phase shifts allow the constraints to be expressed in quadratic form given as

$$\mathbf{X}_{i,k} = \begin{bmatrix} \mathbf{a}_{i,k} \mathbf{a}_{i,k}^H & \mathbf{a}_{i,k} b_{i,k}^H \\ \mathbf{a}_{i,k}^H b_{i,k} & 0 \end{bmatrix}, \ \bar{\boldsymbol{v}} = \begin{bmatrix} \boldsymbol{v} \\ 1 \end{bmatrix}.$$

By using algebraic manipulations, we obtain $\bar{\boldsymbol{v}}^H \mathbf{X}_{i,k} \bar{\boldsymbol{v}} = \text{Tr}(\mathbf{VX})$ where $\mathbf{V} = \bar{\boldsymbol{v}} \bar{\boldsymbol{v}}^H$. The conditions $\mathbf{V} \succeq 0$ and $\text{rank}(\mathbf{V}) = 1$ should be satisfied by $\mathbf{V}$. Since the rank-one constraint is non-convex and makes the problem $(P_{2.2}^*)$ arduous to tackle, we drop this constraint by employing the SDR approach and relax the resultant problem as

$$\left(P_{2.2}^{**}\right) : \max_{\mathbf{V} \in \mathbb{H}^n, \{\beta_k\}_{k=1}^{K_I}} \quad \sum_{k \in K_I} \beta_k \tag{28a}$$

$$\text{s.t. } \text{Tr}(\mathbf{VX}_{k,k}) + |b_{k,k}|^2 \geq \Gamma_{R_{k,\min}}$$

$$\left[\left\{\sum_{i \neq k}^{K_I} \left(\text{Tr}(\mathbf{VX}_{i,k}) + |b_{i,k}|^2\right)\right\} + \sigma_k^2\right] + \beta_k, \tag{28b}$$

$$\text{diag}(\mathbf{V}) = [\mathbf{I}]_{N+1 \times 1}, \tag{28c}$$

$$\mathbf{V} \succeq 0, \quad \beta_k \geq 0, \quad \forall k \in K_I, \tag{28d}$$

where $\mathbf{V} \in \mathbb{H}^n$ guarantees $\mathbf{V} \succeq 0$. $(P_{2.2}^{**})$ is now a standard semi-definite convex programming (SDP) problem that can

Algorithm 1 AO Algorithm for Solving (P2)

Initialization: r: the iteration number, $\xi > 0$: convergence accuracy, $\mathbf{w}_{R_k}^{(0)}$, $\boldsymbol{v}^{(0)}$: initial feasible solutions;
Calculate the initial objective value of problem (P2);
Perform: AO algorithm;
 1. Given $\boldsymbol{v}^{(0)}$, $\mathbf{w}_{R_k}^{(r)}$: Calculate $\mathbf{w}_{R_k}^{(r+1)}$ by solving problem (P$_{2.1}$) with Heuristic Approach;
 2. Given $\mathbf{w}_k^{(r+1)}$ and $\boldsymbol{v}^{(r)}$: Calculate $\boldsymbol{v}^{(r+1)}$ by solving problem (P$_{2.2}^{**}$) with SDR Approach;
   i. Obtain $\mathbf{V}$ by solving (P$_{2.2}^{**}$) using CVX;
   ii. Perform Gaussian randomization to obtain
   $$\bar{\boldsymbol{v}} = \mathbf{U} \sum\nolimits^{\frac{1}{2}} \mathbf{r};$$
   iii. Obtain phase shifts using
   $$\boldsymbol{v} = e^{j\arg}(\bar{\boldsymbol{v}}_{[1:N]}/\bar{\boldsymbol{v}}_{[N+1]});$$
 3. **Update:** transmit beamformers $\mathbf{W}_U^*$, phase shifts $\boldsymbol{v}^*$;
Repeat $r = r + 1$ until (P2) objective value falls below a threshold accuracy i.e., (15a)$\le \xi$.

---

be solved optimally using the MATLAB-based modelling tool CVX for convex optimization [66]. However, (P$_{2.2}^{**}$) does not always provide a rank-one solution, so a Gaussian randomization approach can be used to obtain this solution [54], [57]. In particular, we first perform the eigenvalue decomposition of $\mathbf{V}$ as $\mathbf{V} = \mathbf{U} \sum \mathbf{U}^H$. Afterwards, we obtain the modified solution to (P$_{2.2}^*$) as $\bar{\boldsymbol{v}} = \mathbf{U} \sum^{\frac{1}{2}} \mathbf{r}$, where $\mathbf{r} \sim \mathcal{CN}(0, \mathbf{I}_{N+1}) \in \mathbb{C}^{(N+1) \times 1}$ is a random vector selected from a large number of random generalized circularly symmetric complex Gaussian (CSCG) vectors for maximizing the objective function of (P$_{2.2}^*$). The resultant solution of the problem (P$_{2.2}^*$) is obtained by $\boldsymbol{v}^* = e^{j\arg}(\bar{\boldsymbol{v}}_{[1:N]}/\bar{\boldsymbol{v}}_{[N+1]})$ which satisfies the constraint (27c). The resulting approach offers at least a $\pi/4$-approximation of the optimal values for a particular objective function over a large number of randomizations.

C. COMPUTATIONAL COMPLEXITY ANALYSIS OF AO

Algorithm 1 summarizes the AO algorithm for addressing the problem (P2). The AO method described in Sections III-A and III-B is an iterative, multi-stage optimization algorithm. To optimize transmit beamformers and phase shifts, there are two sub-problems in the outer loop, and each sub-problem needs to be solved using an iterative update approach, respectively. In particular, the MMSE algorithm requires inverse matrix operations with complexity $\mathcal{O}(K_I M^3)$. Additionally, a one-dimensional search (using standard line search) for λ is also required. Therefore, MMSE algorithm complexity is illustrated as $\mathcal{O}(I_\lambda(K_I M^3))$, where I_λ shows the iteration numbers required to find λ. For phase shift optimization, the problem (P$_{2.2}$) optimizes the IRS phase shifts at each iteration by relaxing the SDP problem using an interior point approach. Thus, the computational complexity of the problem (P$_{2.2}$) in solving the SDP problem can be expressed as $\mathcal{O}((N + 1)^{3.5})$ [28]. The total complexity of solving

Algorithm 1 is $\mathcal{O}(I_{out}(I_\lambda(K_I M^3) + I_{inn}(N + 1)^{3.5}))$, where I_{inn} and I_{out} show inner and outer iterations to reach convergence, respectively.

IV. LOW COMPLEXITY ALTERNATIVE SOLUTION

Although the AO approach presented in the above section provides a high-quality converging solution for (P$_{2.2}$), it is computationally complex due to the SDR scheme, and this complexity becomes more significant with increasing number of IRS elements. To alleviate this issue, we propose a low-complexity alternative that decouples the optimization of active beamforming and IRS phase shift design. This strategy takes advantage of IRS's short-range/local coverage, which allows users lying in the vicinity of an IRS-enabled network to receive reflected signals at their respective ends. Accordingly, the IRS phase shifts and transmit beamformers are optimized independently for all users, while adhering to their respective QoS constraints.

A. PHASE SHIFTS OPTIMIZATION

By employing the sum of all users effective IRS channel gains and leveraging the variable changes made in Section IV-B, we reformulate the optimization problem (P$_{2.2}$) and use an iterative approach to solve for phase optimization. The reformulated sub-problem by substituting variables is given by

$$(P_{2.3}) : \max_{\boldsymbol{v}} \quad \sum\nolimits_{k \in K_I} ||(\boldsymbol{v}^H \mathbf{a}_{r,k} + \mathbf{d}_{d,k}^H)||^2 \quad (29a)$$
$$\text{s.t.} \; |v_n| = 1, \quad \forall n \in N, \quad (29b)$$

where $\boldsymbol{v} = [v_1, \ldots, v_N]^H$ for $v_n = e^{j\theta_n}, \forall n \in N$, $\mathbf{a}_{r,k} = \text{diag}(\mathbf{h}_{R_r,k}^H)\mathbf{G}_R \in \mathbb{C}^{1 \times M_U}$, and $\mathbf{g}_{R_d,k}^H = \mathbf{d}_{d,k}^H$. The constraint (15e) is now transformed into a unit-modulus constraint, i.e., $|v_n|^2 = 1, \forall n$. (P$_{2.3}$) is still a non-convex optimization problem due to constraint (29b). However, the phase optimization can be solved by an iterative method due to the fully separable phase shifts in constraint (29b). Thus, we exploit low complexity EBCD approach for solving (P$_{2.3}$) by iteratively optimizing each element of $\boldsymbol{v}$, i.e., v_n ($\forall n \in N$) given the other phase shifts, v_l ($\forall l \in N$) where $l \neq n$ as fixed. The sub-problem is presented as

$$\left(P_{2.3}^*\right) : \max_{\boldsymbol{v}} \quad f(\boldsymbol{v}) \quad (30a)$$
$$\text{s.t.} \; |v_n| = 1, \; \forall n \in N. \quad (30b)$$

With fixed v_l, (P$_{2.3}$) becomes a linear objective function given as

$$f(\boldsymbol{v}) = \sum_{l \neq n}^{N} v_l \mathbf{Q}(l,l)v_l^H + 2\mathbb{R}\{v_n \vartheta_n\} + S \quad (31)$$

where

$$\mathbf{Q} = \sum_k \mathbf{a}_{r,k} \mathbf{a}_{r,k}^H, \; \forall k \in K_I, \quad (32)$$

$$\vartheta_n = \sum_{l \neq n}^{N} \mathbf{Q}(n,l)v_l^H - \tilde{\boldsymbol{\vartheta}}(n), \quad (33)$$

Algorithm 2 EBCD Algorithm for Solving (P$_{2.3}$)

Input: $\boldsymbol{v}_n^{(0)}$: initial feasible solution, r: iteration number, $\xi > 0$: convergence accuracy;
Output: Optimal solution, i.e., $\boldsymbol{v}_n^*$;
Solve: Objective function, i.e., $f(\boldsymbol{v}_n^{(0)})$;
Repeat
  for $r = r + 1$ **do**
    for $n = 1$ to N **do**
      1. Solve (37) to calculate optimal $\boldsymbol{v}_n^*$ $\{\forall n \in N\}$, for fixed v_l $\{\forall l \in N\}, l \neq n$;
      2. Obtain $\boldsymbol{v}_n^* = \{\boldsymbol{v}_1^*, \ldots, \boldsymbol{v}_l^*, \ldots, \boldsymbol{v}_N^*\}$
      3. Set $\boldsymbol{v}_n^{(r+1)} = \boldsymbol{v}_n^*$ and calculate $f(\boldsymbol{v}_n^{(r+1)})$;
      4. Perform iterations till stopping criteria meets i.e.,

$$\frac{||f(v_n^{(r+1)}) - f(v_n^{(r)})||}{f(v_n^{(r+1)})} < \xi;$$

    end
  end
until convergence;

$$\tilde{\boldsymbol{\vartheta}} = \sum_k \mathbf{a}_{\mathrm{r},k} \mathbf{d}_{\mathrm{d},k}^H, \quad \forall k \in K_\mathrm{I}. \tag{34}$$

$$S = \mathbf{Q}(n,n) - 2\mathbb{R}\sum_{l \neq n}^N v_l \tilde{\boldsymbol{\vartheta}}(l) + \sum_k |\mathbf{d}_{\mathrm{d},k}^H|^2, \quad \forall k \in K_\mathrm{I}. \tag{35}$$

By dropping constant term S from (31) and taking into account the unit-modulus constraint with some algebraic properties, the sub-problem (P$_{2.3}^*$) becomes the given update rule,

$$\left(\mathrm{P}_{2.3}^{**}\right) : \max_{\boldsymbol{v}_n} \ 2\mathbb{R}\{v_n \vartheta_n\} \tag{36a}$$
$$\text{s.t.} \ |v_n| = 1, \ \forall n \in N. \tag{36b}$$

Consequently, by fixing v_l $\{\forall l \in N\}, l \neq n$ the optimal solution to (P$_{2.3}^{**}$) becomes

$$v_n^* = \begin{cases} 1, \text{if } v_n = 0, \\ \frac{-\vartheta_n^H}{|\vartheta_n|}, \ \forall n \in N, \text{otherwise.} \end{cases} \tag{37}$$

According to (37), each block of $N-1$ phase shifts can be optimized iteratively by fixing the other N phases until the convergence is achieved in this block, which is implied by the fractional decrease in (P$_{2.3}^*$) objective function value below a positive tolerance threshold. Algorithm 2 summarizes the EBCD method for solving problem (P$_{2.2}$) to obtain optimal phase shifts.

B. TRANSMIT BF OPTIMIZATION

By exploiting phase shifts obtained from Algorithm 1, the effective channels of U^{net} users can be modeled easily. Further, at the AP$_\mathrm{U}$ without phase shifts consideration, the transmit BF is performed for the given channel models by solving the following sub-problem

$$(\mathrm{P}_{2.4}) : \min_{\mathbf{W}_\mathrm{U}} \ \sum_{k=1}^{K_\mathrm{I}} ||\mathbf{w}_{\mathrm{R}_k}||^2 \tag{38a}$$

Algorithm 3 Overall Low Complexity Alternative Algorithm for Solving (P$_2$)

Initialization: r: the iteration number, $\xi > 0$: convergence accuracy, $\mathbf{w}_{\mathrm{R}_k}^{(0)}$, $\boldsymbol{v}^{(0)}$: initial feasible solutions;
Repeat
  1. Update IRS phase shifts by solving (P$_{2.3}$).
  2. Update transmit beamformers by solving (P$_{2.4}$).
  3. Perform iterations until the objective value of (P$_2$) falls below threshold accuracy i.e., (15a)$\leq \xi$.
until convergence;

$$\text{s.t.} \ \Gamma_{\mathrm{R}_k} \geq \Gamma_{\mathrm{R}_{k,\min}}, \ \forall k \in K_\mathrm{I}, \tag{38b}$$

(P$_{2.4}$) is similar to (P$_2$) without considering IRS phase shifts. The problem can be solved feasibly using Heuristic approach discussed in Section IV-A.

C. COMPUTATIONAL COMPLEXITY ANALYSIS OF ALTERNATIVE SOLUTION

Algorithm 3 outlines the proposed low-complexity algorithm for solving the (P$_2$) optimization problem. This alternative approach offers closed-form solutions for the optimization variables, significantly enhancing computational efficiency. By decoupling the optimization variables in (P$_{2.3}$) and (P$_{2.4}$) and solving them independently, the overall complexity is substantially reduced, making the method particularly suitable for large-scale IRS deployments with a growing number of elements. Specifically, the computational complexity of solving (P$_{2.3}$) is $\mathcal{O}(I_0 N)$, where I_0 denotes the number of iterations required for convergence. For (P$_{2.4}$), which is solved using the MMSE technique, the complexity is $\mathcal{O}(K_\mathrm{I} M^3)$. Consequently, the overall computational complexity for jointly solving (P$_{2.3}$) and (P$_{2.4}$) is given by $\mathcal{O}(I_{\mathrm{out}}(I_\lambda(K_\mathrm{I} M^3) + I_{\mathrm{inn}} N))$, where I_{inn} and I_{out} represent the number of inner and outer iterations, respectively, required to achieve convergence.

V. EE OPTIMIZATION AT I^{NET}

The problem of phase shifts optimization is solved in Sections III-B and IV-A by exploiting the SDP approach using SDR and an iterative solution via EBCD methods, respectively. By exploiting these phase shifts of U^{net} using the phase cooperation approach, the problem of EE maximization at I^{net} can be feasibly solved. In this section, we first optimize the EH coefficient (φ_k) of I^{net} by deriving a closed-form solution that can effectively improve the resultant EE. For a given BF vector and by employing phase shifts of U^{net}, the optimization problem (P$_1$) will become

$$(\mathrm{P}_{1.1}) : \max_{\varphi} \ \frac{\mathcal{R}_k^{\mathrm{I}^{net}}}{1/\eta \sum_{k=1}^{K_\mathrm{E+I}} ||\mathbf{w}_{\mathrm{D}_k}||^2 + P_C} \tag{39a}$$
$$\text{s.t.} \ (14b), \ (14d), \ (14g) \tag{39b}$$

To solve (P$_{1.1}$) a closed-form solution for φ_k is derived by using the achievable data rate constraint of I^{net} given as

$$\mathcal{R}_{\mathrm{D}_k} > \mathcal{R}_{\mathrm{D}_{k,\min}}, \quad \forall k \in K_{\mathrm{E+I}}, \tag{40}$$

where $\mathcal{R}_{D_{k,min}}$ is the minimum predefined data rate. Since D_k can only decode data when (40) is met. Consequently, the EH coefficient obtained by solving (40) is the optimized φ_k, and it is given by

$$\varphi_k = 1 - \frac{\Gamma_{D_{k,min}} \sigma_k^2}{|\mathbf{f}_{D_k}^H \mathbf{w}_{D_k}|^2 - \Gamma_{D_{k,min}} \sum_{j \neq k} |\mathbf{f}_{D_k}^H \mathbf{w}_{D_j}|^2} - \epsilon. \quad (41)$$

Proof: Please, refer to the Appendix. ∎

By defining a pre-threshold $\bar{E}_{\mathcal{H}_k}$ and using (41), the constraint (14b) can be easily satisfied. Next, by substituting optimize φ_k in (P$_1$), the resultant problem can be simplified to a transmit BF optimization similar to (P$_{2.1}^*$), which can be feasibly solved by using Section III-A heuristic approach.

VI. SIMULATION RESULTS AND DISCUSSION

In this section, we present numerical results to evaluate the performance of the proposed framework and optimization schemes. The performance is assessed by considering EE maximization for both users and PS-SWIPT based SS-IoT networks. The channel model is created based on the 3GPP propagation environment, and we adopt the simulation parameters from various existing works [27], [34], [35]. We consider two APs, AP$_U$ and AP$_I$, equipped with multiple antennas for serving U^{net} and I^{net}, whereas within each network we consider 6 users and 6 SS-IoT devices equipped with single antennas and distributed randomly in a circular region centered at $(10, 0)$ with radius $r_{\{U, I\}} = 6$ m separately. The APs are located at $(0; 0; 0)$, and the IRS is deployed at a location of $(X_{IRS} = 6$ m; $Y_{IRS} = 8$ m; 0). For further simulation setup, the 3-D coordinate system with network deployment is shown in Fig. 2. The channel links between the APs-IRS and IRS to U^{net} and I^{net} are mutually independent; hence, we adopt a line-of-sight (LoS) channel model, i.e., the Rician fading model for APs-IRS, whereas the channel links between the IRS to U^{net} and I^{net} follow Rayleigh distribution as the users and devices are deployed randomly. For the considered framework, the path loss channel model is designed according to the 3GPP propagation environment, and the channel model is expressed as

$$\mathbf{G}_{R,D} = \sqrt{P(L_x)} \left\{ \sqrt{\frac{\kappa}{1+\kappa}} \mathbf{G}^{LoS} + \sqrt{\frac{\kappa}{1+\kappa}} \mathbf{G}^{NLoS} \right\}, \quad (42)$$

$$\mathbf{h}_{\{R,D\}_{r,k}}^H = \sqrt{P(L_x)} \left\{ \sqrt{\frac{\kappa}{1+\kappa}} \mathbf{h}_{\{R,D\}_{r,k}}^{H(LoS)} \right.$$
$$\left. + \sqrt{\frac{1}{1+\kappa}} \mathbf{h}_{\{R,D\}_{r,k}}^{H(NLoS)} \right\}, \quad (43)$$

$$\mathbf{g}_{\{R,D\}_{d,k}}^H = \sqrt{P(L_x)} \mathbf{g}_{\{R,D\}_{d,k}}^H. \quad (44)$$

Here, $P(L_x)$ is the distance dependent path-loss model given by $P(L_x) = C_0 (d_x/d_0)^{-a_x}$, where C_0 is the path loss at the reference distance d_0, d_x, and a_x $\forall x \in \{$APs-IRS, IRS $-$ R$_k$, D$_k$, APs $-$ R$_k$, D$_k\}$ shows the distances and path loss exponents of the individual links, respectively. Whereas, $a_{\text{APs-IRS}} = 2$, $a_{\text{IRS-R}_k,D_k} = 2.5$, and $a_{\text{APs-R}_k,D_k} = 3.5$ show
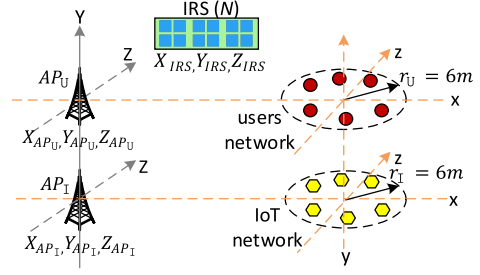

FIGURE 2. 3D-setup for network deployment.

their respective path losses. For the proposed network model under consideration, we consider a bandwidth of 1 MHz and noise variance σ_k^2, $\forall k \in \{$U, I$\}$. Moreover, we consider $\kappa = 5$ dB as the Rician constant factor, $\mathbf{G}^{LoS}$, $\mathbf{h}_{\{R,D\}_{r,k}}^{H(LoS)}$, and $\mathbf{G}^{NLoS}$, $\mathbf{h}_{\{R,D\}_{r,k}}^{H(NLoS)}$ represent the LoS and non-LoS (NLoS) components of reflected paths, respectively. The elements of $\mathbf{G}^{NLoS}$ and $\mathbf{h}_{\{R,D\}_{r,k}}^{H(NLoS)}$ follow the Rayleigh fading model with identical independent distribution (i.i.d.). The channel coefficients for the direct path, i.e., without the IRS scenario $\mathbf{g}_{\{R,D\}_{d,k}}^H$ are generated at random from a Gaussian normal distribution. Furthermore, we consider that all users and IoT devices have the same SINR requirements, i.e., $\Gamma_{\{R,D\}_{k,min}} = 4$ dB, $\forall k$. Some other parameters we consider are $\eta_{\{R,D\}_k} = 0.8$, $P_{C_{\{U, I\}}} = 5$ dBm, $\mu_{D_k} = 0.8$, and $\epsilon_{D_k} = 10^{-5}$.

The simulation results for the proposed framework are evaluated based on the following baseline schemes.

- **Baseline Scheme 1 (AO with IRS):** The maximization problem is solved for U^{net} using transmit BF and phase shifts optimization by applying AO with IRS. The BF vectors are optimized using heuristic approach whereas the phase shifts are optimized via computationally efficient SDR scheme. The CVX tool [66] is used to solve the phase optimization, with threshold accuracy and line-search accuracy set to $\xi_{\{U,I\}} = 0.001$ and $\zeta_{\{U,I\}} = 0.1$, respectively. For the proposed approach, we consider 10000 Gaussian randomizations for. The EE maximization is then performed for I^{net} by using the heuristic BF algorithm and the U^{net} optimal phase shifts Θ.

- **Baseline Scheme 2 (Low Complexity Alternative Solution with IRS (LCAS)):** The phase shifts and BF vectors are optimized via low complexity alternative solution. For IRS phase optimization, EBCD approach with 3000 iterations and a convergence accuracy of $\xi = 0.001$ is used.

- **Baseline Scheme 3 (Discrete IRS Phase Shifts (DPS)):** A discrete set of IRS phase shifts is considered by using the approaches of [67] and [35]. The optimal discrete phases are obtained as $v_n^* = exp(j\beta_{n, l^*})$ $\forall n \in \{1, N\}, \forall l^* \in \{1, \mathcal{L}\}$, where $\mathcal{L} = 2^{\mathcal{B}_0}$ shows the total number of discrete phase shifts, and $\mathcal{B}_0$ represent the IRS phase resolution bits. The optimal set of DPS are selected from SDR or EBCD approach for employing phase optimization.
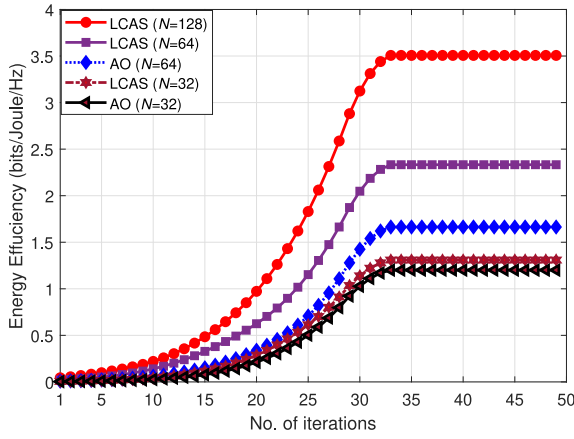
FIGURE 3. Convergence behaviour of Algorithms 1 and 3.

FIGURE 4. Sum rate versus P_{AP_U}.

FIGURE 5. Energy efficiency versus P_{AP_U}.

- **Baseline Scheme 4 (Random IRS phase shifts (RPS)):** The phase shifts of IRS are randomly generated, and the BF optimization is performed by heuristic schemes. For SWIPT network PS ratio is obtained via closed-form expression.
- **Baseline Scheme 5 (Without IRS (W/O IRS)):** The system model is reduced to conventional wireless PS-SWIPT based I^{net} without IRS support. The APs employ a direct communication link in the presence of obstacles, considering the practical path loss channel model.
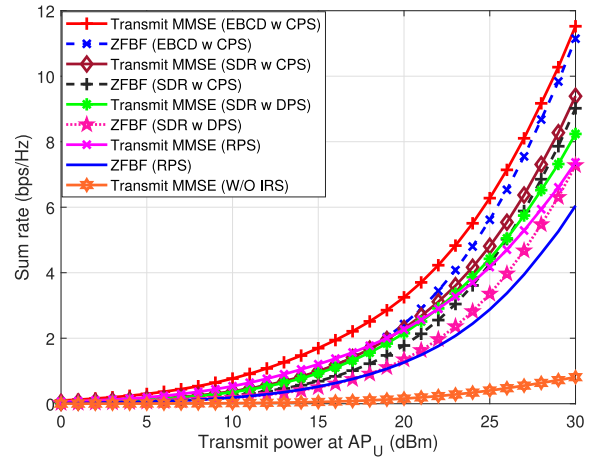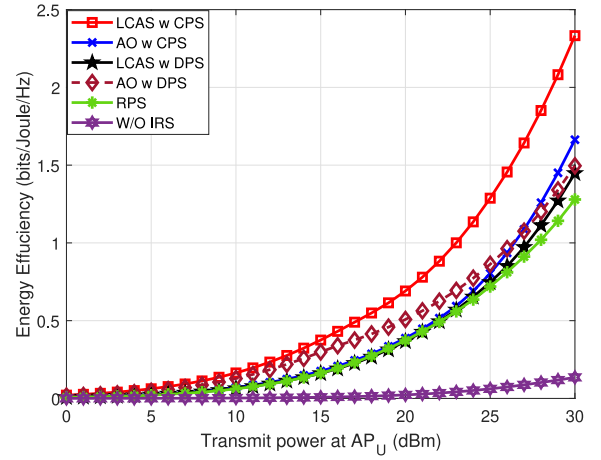
To benchmark the performance of MMSE scheme, we also analyze rate curves of above baseline schemes using ZFBF method discussed in Section III-A.

A. CONVERGENCE ANALYSIS OF ALGORITHM 1 and 3

First, we analyze the convergence behavior of algorithms 1 and 3 with continuous phase shifts as presented in Fig. 3. We analyze the EE performance curves versus iteration numbers for the discussed framework using a fixed number of APs antennas and varying IRS reflection elements, i.e., $M_U = 10$ and $N = 32, 64,$ and 128, respectively. The performance curves in Fig. 3 prove the convergence of the AO and the LCAS algorithms, clearly indicating that after a few iterations, the EE curve shows stable convergence behavior at a single point, thus confirming the convergence of both algorithms. It is also noteworthy that when the algorithms converge, they achieve a relatively similar performance at a small number of IRS elements, validating the theoretical and computational analysis discussed in Sections III-B and IV-A for Algorithms 1 and 3.

B. PERFORMANCE ANALYSIS OF U^{NET}

For the proposed PC_{Net}, the optimal phase shifts of U^{net} are exploited by I^{net} to improve the EE performance without constraining resources. Hence, we first investigate the performance of U^{net} from some aspects with the outlined baseline schemes. The sum rate and EE performance metrics are plotted against the maximum transmit power, i.e., P_{AP_U}

at AP_U, respectively, in Figures 4 and 5. As expected, with increasing P_{AP_U}, both the sum rate and EE curves show an increasing trend. By employing Algorithms 1 and 3, the curve achieves a significant performance gain compared to other baseline schemes. Furthermore, it is noted that the proposed scheme with continuous phase shifts (CPS) and DPS performs better than RPS and W/O IRS approaches, which confirms that IRS can improve the performance of the WIT networks. For transmit BF comparison, it is shown from gain curves that ZFBF is asymptotically ideal at high values of transmit power, whereas transmit MMSE BF achieves higher performance than ZFBF through the entire range of transmit power; however, MMSE performance relies strongly on careful adjustment of the controlling parameter λ_k.

Next, we investigate the EE performance vs. the number of IRS reflection elements N, which can be easily observed to have a monotonically increasing trend as shown in Fig. 6. With increasing N, the respective energy and information signals become stronger at the intended receiver end; hence, the EE performance of all baseline schemes shows improvement compared to the W/O IRS case, and the performance of proposed Algorithms 1 and 3 outperforms other schemes.
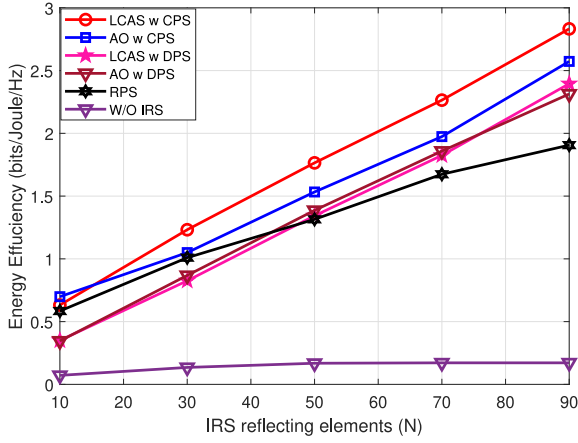
FIGURE 6. Energy efficiency versus reflecting elements *N*.

Moreover, even the EE curve when employing the RPS scheme also shows higher EE performance than the W/O IRS scheme, particularly with large *N*, implying that the IRS can bring a substantial rise in the performance gain of conventional networks. Moreover, it supports the utilization of IRS in place of active antennas and expensive RF modules to reduce system costs.

C. PERFORMANCE ANALYSIS OF $\mathtt{I}^{NET}$

In this section, by exploiting the optimal phase shifts of $\mathtt{U}^{net}$ obtained via SDR and EBCD approaches, the EE performance is evaluated for a PS-SWIPT based SS-IoT network via effective phase cooperation. For the given optimal phase shifts and optimal PS coefficients, the EE curves vs. maximum transmit power available at $P_{\mathrm{AP_I}}$ are shown in Fig. 7 for the considered baseline schemes. As expected from $\mathtt{U}^{net}$ results, the EE of $\mathtt{I}^{net}$ also rises with an increasing $P_{\mathrm{AP_I}}$ trend. By employing a heuristic BF approach for the given optimal Θ and φ_k, the EE curves of $\mathtt{I}^{net}$ achieve a significant performance gain compared with the W/O IRS scheme, which confirms that using IRS phase cooperation we can enhance SWIPT IoT networks performance.

Next, we unveil the potential of the varying IRS elements of $\mathtt{U}^{net}$ on the EE performance of $\mathtt{I}^{net}$ in Fig. 7. We consider different IRS reflecting elements for optimizing $\mathtt{U}^{net}$ Θ and exploiting these constant optimal phase shifts via phase cooperation; EE curves are evaluated for $\mathtt{I}^{net}$. The performance curves validate the effectiveness of phase cooperation with a monotonically increasing trend, as shown in Fig. 7 results. Again, the EE achieved by the baseline scheme increases compared to the W/O IRS phase cooperation case. This implies that with improved phase shifts, a substantial rise in performance gains for PS-SWIPT based SS-IoT networks can be achieved.

Fig. 8 shows the PS-SWIPT network EE performance against the overall circuit power consumption P_C at $\mathrm{AP_I}$. We set transmit antennas at $M_I = 10$, exploit phase shifts with $N = 64$, and P_C ranges from 0 to 15 dBm. Further, we considered a different transmit power budget for the proposed scheme. Fig. 8 curves demonstrate that the EE declines when
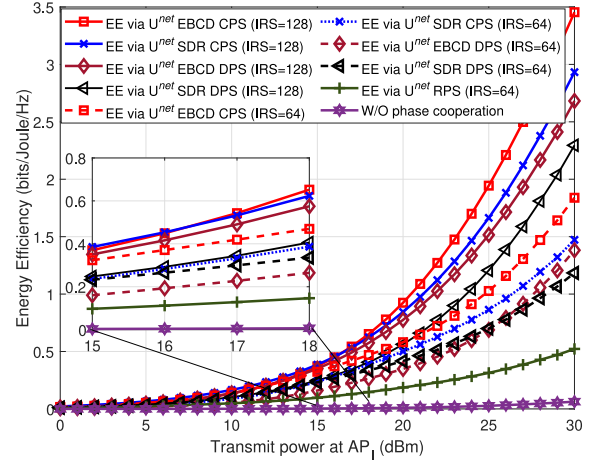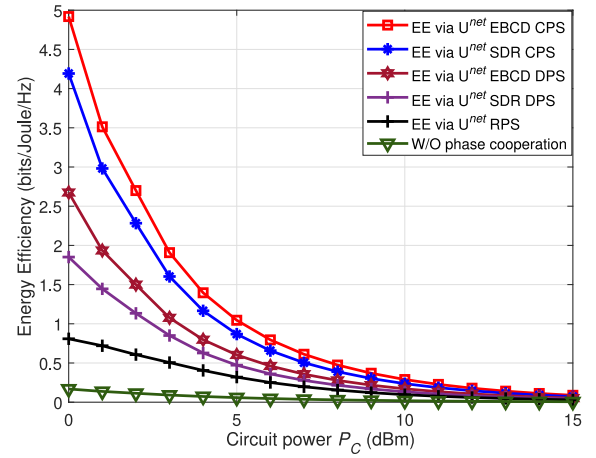

FIGURE 7. Energy efficiency versus $P_{\mathrm{AP_I}}$.

FIGURE 8. Energy efficiency versus P_C at $\mathtt{I}^{net}$.
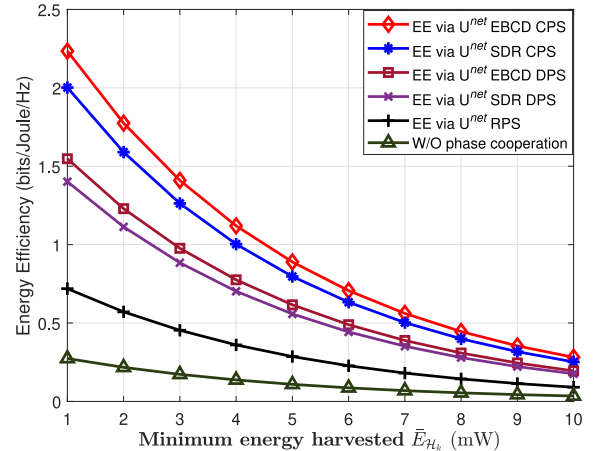

FIGURE 9. Energy efficiency versus minimum energy harvested by D_k for information decoding.

the circuit power increases, which is consistent with the EE maximization principle. However, as P_C further increases, the slope of the declining curve decreases since optimization is more prevalent in increasing network EE when P_C is low. The performance of EE curves with phase cooperation outperforms those without phase cooperation.

Finally we illustrate the EE versus minimum energy harvested requirement of SS-IoT devices, i.e., $\bar{E}_{\mathcal{H}_k}$ using the baseline schemes in Fig. 9. As we can see, the proposed solution with phase cooperation outperforms the benchmarks significantly. Besides, IRS-enabled phase cooperative systems are more resistant to minimum energy harvested than conventional systems, as demonstrated by the difference between the scheme with optimal phase shifts and the scheme without phase shifts with increasing minimum harvested energy.

VII. CONCLUSION AND FUTURE WORK

This article investigated a novel IRS-enabled PS-SWIPT based SS-IoT phase cooperative framework with the formulation of the EE maximization problem for designing optimal transmission BF vectors, IRS phase shifts, and PS coefficients. To solve the non-convex optimization problem, first we applied an AO to the user network to derive transmit BF vectors using closed-form heuristic solutions and optimal phase shifts using a relaxed SDP scheme. Furthermore, we have proposed an alternative solution of lower complexity by decoupling the original optimization problem into subproblems to obtain the optimal phase shifts through an iterative EBCD approach and transmit beamformers using a heuristic scheme. Later, the EE maximization problem is solved for the SS-IoT network by optimizing PS coefficients and exploiting optimal phase shifts of the users network via a phase cooperation approach. A quantitative comparison of the proposed framework with the baseline schemes shows that the proposed framework can achieve high EE benefits at a low level of complexity. Further, the proposed framework can significantly reduce hardware costs by deploying IRS in conventional networks. With multiple IRSs-aided phase cooperative networks, the proposed framework can be feasibly extended in the future to a multi-user MIMO SS-IoT network scenario. Future research may investigate hierarchical and distributed optimization strategies to further improve the scalability of the proposed phase-cooperative framework, particularly in the context of large-scale IoT network deployments. Additionally, the performance of the considered network can be further analyzed by employing heuristic methods and stochastic gradient descent techniques for phase optimization under imperfect CSI conditions.

APPENDIX
A. DERIVATION OF OPTIMIZED EH COEFFICIENT
By substituting achievable rate expression in (40) we obtained

$$\log_2\left(1 + \Gamma_{\mathrm{D}_k}^{\mathrm{ID}}\right) \geq \mathcal{R}_{\mathrm{D}_{k,\min}}, \quad \forall k \in K_{\mathrm{E+I}}. \quad (45)$$

Substituting SINR from (9) we have

$$\log_2\left(1 + \frac{(1-\varphi_k)|\left(\mathbf{h}_{\mathrm{D}r,k}^H \Theta \mathbf{G}_{\mathrm{D}} + \mathbf{g}_{\mathrm{D}d,k}^H\right)\mathbf{w}_{\mathrm{D}_k}|^2}{\sum_{j\neq k}(1-\varphi_k)|\left(\mathbf{h}_{\mathrm{D}r,k}^H \Theta \mathbf{G}_{\mathrm{D}} + \mathbf{g}_{\mathrm{D}d,k}^H\right)\mathbf{w}_{\mathrm{D}_j}|^2 + \sigma_k^2}\right)$$
$$\geq \mathcal{R}_{\mathrm{D}_{k,\min}}. \quad (46)$$

Let us substitute $\mathbf{f}_{\mathrm{D}_k}^H = (\mathbf{h}_{\mathrm{D}r,k}^H \Theta \mathbf{G}_{\mathrm{D}} + \mathbf{g}_{\mathrm{D}d,k}^H)$ for simplification of representation

$$\left(\frac{(1-\varphi_k)|\mathbf{f}_{\mathrm{D}_k}^H \mathbf{w}_{\mathrm{D}_k}|^2}{\sum_{j\neq k}(1-\varphi_k)|\mathbf{f}_{\mathrm{D}_k}^H \mathbf{w}_{\mathrm{D}_j}|^2 + \sigma_k^2}\right) \geq 2^{\mathcal{R}_{\mathrm{D}_{k,\min}}} - 1, \quad (47)$$

$$\left(\frac{(1-\varphi_k)|\mathbf{f}_{\mathrm{D}_k}^H \mathbf{w}_{\mathrm{D}_k}|^2}{\sum_{j\neq k}(1-\varphi_k)|\mathbf{f}_{\mathrm{D}_k}^H \mathbf{w}_{\mathrm{D}_j}|^2 + \sigma_k^2}\right) \geq \Gamma_{\mathrm{D}_{k,\min}}, \quad (48)$$

where $\Gamma_{\mathrm{D}_{k,\min}}$ is the minimum SINR.

$$(1-\varphi_k)|\mathbf{f}_{\mathrm{D}_k}^H \mathbf{w}_{\mathrm{D}_k}|^2 \geq \Gamma_{\mathrm{D}_{k,\min}}\left(\sum_{j\neq k}(1-\varphi_k)|\mathbf{f}_{\mathrm{D}_k}^H \mathbf{w}_{\mathrm{D}_j}|^2 + \sigma_k^2\right), \quad (49)$$

$$(1-\varphi_k)|\mathbf{f}_{\mathrm{D}_k}^H \mathbf{w}_{\mathrm{D}_k}|^2 - \Gamma_{\mathrm{D}_{k,\min}}\sum_{j\neq k}(1-\varphi_k)|\mathbf{f}_{\mathrm{D}_k}^H \mathbf{w}_{\mathrm{D}_j}|^2$$
$$\geq +\Gamma_{\mathrm{D}_{k,\min}}\sigma_k^2, \quad (50)$$

$$(1-\varphi_k) \geq \frac{\Gamma_{\mathrm{D}_{k,\min}}\sigma_k^2}{|\mathbf{f}_{\mathrm{D}_k}^H \mathbf{w}_{\mathrm{D}_k}|^2 - \Gamma_{\mathrm{D}_{k,\min}}\sum_{j\neq k}|\mathbf{f}_{\mathrm{D}_k}^H \mathbf{w}_{\mathrm{D}_j}|^2}, \quad (51)$$

$$\varphi_k \leq 1 - \frac{\Gamma_{\mathrm{D}_{k,\min}}\sigma_k^2}{|\mathbf{f}_{\mathrm{D}_k}^H \mathbf{w}_{\mathrm{D}_k}|^2 - \Gamma_{\mathrm{D}_{k,\min}}\sum_{j\neq k}|\mathbf{f}_{\mathrm{D}_k}^H \mathbf{w}_{\mathrm{D}_j}|^2}. \quad (52)$$

To ensure that φ_k always satisfy the condition mentioned in (52), we introduce a new small slack variables ϵ such that (52) becomes

$$\varphi_k = 1 - \frac{\Gamma_{\mathrm{D}_{k,\min}}\sigma_k^2}{|\mathbf{f}_{\mathrm{D}_k}^H \mathbf{w}_{\mathrm{D}_k}|^2 - \Gamma_{\mathrm{D}_{k,\min}}\sum_{j\neq k}|\mathbf{f}_{\mathrm{D}_k}^H \mathbf{w}_{\mathrm{D}_j}|^2} - \epsilon. \quad (53)$$

REFERENCES

[1] W. Shi, W. Xu, X. You, C. Zhao, and K. Wei, "Intelligent reflection enabling technologies for integrated and green Internet-of-Everything beyond 5G: Communication, sensing, and security," *IEEE Wireless Commun.*, vol. 30, no. 2, pp. 147–154, Apr. 2023.

[2] H. Sadia, A. K. Hassan, Z. H. Abbas, G. Abbas, and J. M. Cioffi, "An IRS-Enabled phase cooperative framework for sum rate maximization in B5G networks," *IEEE Trans. Netw. Sci. Eng.*, vol. 12, no. 1, pp. 134–144, Jan./Feb. 2025.

[3] J. Iannacci, "Point of view: A perspective vision of Micro/Nano systems and technologies as enablers of 6G, super-IoT, and tactile Internet," *Proc. IEEE*, vol. 111, no. 1, pp. 5–18, Jan. 2023.

[4] Y. Liu, H.-N. Dai, Q. Wang, M. Imran, and N. Guizani, "Wireless powering Internet of Things with UAVs: Challenges and opportunities," *IEEE Netw.*, vol. 36, no. 2, pp. 146–152, Mar./Apr. 2022.

[5] A. Elsts et al., "Enabling healthcare in smart homes: The SPHERE IoT network infrastructure," *IEEE Commun. Mag.*, vol. 56, no. 12, pp. 164–170, Dec. 2018.

[6] M. Vaezi et al., "Cellular, wide-area, and non-terrestrial IoT: A survey on 5G advances and the road toward 6G," *IEEE Commun. Surveys Tuts.*, vol. 24, no. 2, pp. 1117–1174, 2nd Quart., 2022.

[7] B. Clerckx, R. Zhang, R. Schober, D. W. K. Ng, D. I. Kim, and H. V. Poor, "Fundamentals of wireless information and power transfer: From RF energy harvester models to signal and system designs," *IEEE J. Sel. Areas Commun.*, vol. 37, no. 1, pp. 4–33, Jan. 2019.

[8] T. D. P. Perera, D. N. K. Jayakody, S. K. Sharma, S. Chatzinotas, and J. Li, "Simultaneous wireless information and power transfer (SWIPT): Recent advances and future challenges," *IEEE Commun. Surveys Tuts.*, vol. 20, no. 1, pp. 264–302, 1st Quart., 2018.

[9] H. Liu, K. J. Kim, K. S. Kwak, and H. V. Poor, "Power splitting-based SWIPT with decode-and-forward full-duplex relaying," *IEEE Trans. Wireless Commun.*, vol. 15, no. 11, pp. 7561–7577, Nov. 2016.

[10] K. W. Choi et al., "Simultaneous wireless information and power transfer (SWIPT) for Internet of Things: Novel receiver design and experimental validation," *IEEE Internet Things J.*, vol. 7, no. 4, pp. 2996–3012, Apr. 2020.
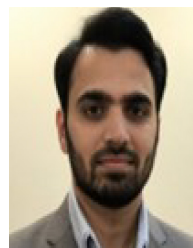
[11] J. Fang, C. Zhang, Q. Wu, and A. Li, "Improper Gaussian signaling for IRS assisted multiuser SWIPT systems with hardware impairments," *IEEE Trans. Veh. Technol.*, vol. 72, no. 10, pp. 13024–13038, Oct. 2023.

[12] D. Xu, V. Jamali, X. Yu, D. W. K. Ng, and R. Schober, "Optimal resource allocation design for large IRS-assisted SWIPT systems: A scalable optimization framework," *IEEE Trans. Commun.*, vol. 70, no. 2, pp. 1423–1441, Feb. 2022.

[13] X. Xie et al., "A joint optimization framework for IRS assisted energy self sustainable IoT networks," *IEEE Internet Things J.*, vol. 9, no. 15, pp. 13767–13779, Aug. 2022.

[14] Q. Shi, L. Liu, W. Xu, and R. Zhang, "Joint transmit beamforming and receive power splitting for MISO SWIPT systems," *IEEE Trans. Wireless Commun.*, vol. 13, no. 6, pp. 3269–3280, Jun. 2014.

[15] J. Wang, G. Wang, B. Li, H. Yang, Y. Hu, and A. Schmeink, "Massive MIMO two-way relaying systems with SWIPT in IoT networks," *IEEE Internet Things J.*, vol. 8, no. 20, pp. 15126–15139, Oct. 2021.

[16] H. Sadia et al., "IRS-enabled NOMA communication systems: A network architecture primer with future trends and challenges," *Digit. Commun. Netw.*, vol. 10, no. 5, pp. 1503–1528, 2024.

[17] Q. Liu, S. Sun, B. Rong, and M. Kadoch, "Intelligent reflective surface based 6G communications for sustainable energy infrastructure," *IEEE Wireless Commun.*, vol. 28, no. 6, pp. 49–55, Dec. 2021.

[18] Y. Cheng, W. Peng, and T. Jiang, "Self-sustainable RIS aided wireless power transfer scheme," *IEEE Trans. Veh. Technol.*, vol. 72, no. 1, pp. 881–892, Jan. 2023.

[19] C. Pan et al., "Multicell MIMO communications relying on intelligent reflecting surfaces," *IEEE Trans. Wireless Commun.*, vol. 19, no. 8, pp. 5218–5233, Aug. 2020.

[20] Q. Wu, S. Zhang, B. Zheng, C. You, and R. Zhang, "Intelligent reflecting surface-aided wireless communications: A tutorial," *IEEE Trans. Commun.*, vol. 69, no. 5, pp. 3313–3351, May 2021.

[21] M. D. Renzo et al., "Reconfigurable intelligent surfaces vs. Relaying: Differences, similarities, and performance comparison," *IEEE Open J. Commun. Soc.*, vol. 1, pp. 798–807, 2020.

[22] H. Sadia, A. K. Hassan, Z. H. Abbas, and G. Abbas, "System throughput maximization in IRS-assisted phase cooperative NOMA networks," *Phys. Commun.*, vol. 58, Jun. 2023, Art. no. 102007.

[23] W. Mei, B. Zheng, C. You, and R. Zhang, "Intelligent reflecting surface-aided wireless networks: From single-reflection to multi-reflection design and optimization," *Proc. IEEE*, vol. 110, no. 9, pp. 1380–1400, Sep. 2022.

[24] H. Sadia, H. Iqbal, S. F. Hussain, and N. Saeed, "Signal detection in intelligent reflecting surface-assisted NOMA network using LSTM model: A ML approach," *IEEE Open J. Commun. Soc.*, vol. 6, pp. 29–38, 2025.

[25] Z. Li, W. Chen, Q. Wu, K. Wang, and J. Li, "Joint beamforming design and power splitting optimization in IRS-assisted SWIPT NOMA networks," *IEEE Trans. Wireless Commun.*, vol. 21, no. 3, pp. 2019–2033, Mar. 2021.

[26] R. Ma, J. Tang, X. Zhang, K.-K. Wong, and J. A. Chambers, "Energy efficiency optimization for mutual-coupling-aware wireless communication system based on RIS-enhanced SWIPT," *IEEE Internet Things J.*, vol. 10, no. 22, pp. 19399–19414, Nov. 2023.

[27] Q. Wu and R. Zhang, "Weighted sum power maximization for intelligent reflecting surface aided SWIPT," *IEEE Wireless Commun. Lett.*, vol. 9, no. 5, pp. 586–590, May 2020.

[28] Q. Wu and R. Zhang, "Joint active and passive beamforming optimization for intelligent reflecting surface assisted SWIPT under QoS constraints," *IEEE J. Sel. Areas Commun.*, vol. 38, no. 8, pp. 1735–1748, Aug. 2020.

[29] Q. Wu, X. Zhou, W. Chen, J. Li, and X. Zhang, "IRS-aided WPCNs: A new optimization framework for dynamic IRS beamforming," *IEEE Trans. Wireless Commun.*, vol. 21, no. 7, pp. 4725–4739, Jul. 2022.

[30] C. Pan et al., "Intelligent reflecting surface aided MIMO broadcasting for simultaneous wireless information and power transfer," *IEEE J. Sel. Areas Commun.*, vol. 38, no. 8, pp. 1719–1734, Aug. 2020.

[31] Y. Lu, K. Xiong, P. Fan, Z. Ding, Z. Zhong, and K. B. Letaief, "Global energy efficiency in secure MISO SWIPT systems with non-linear power-splitting EH model," *IEEE J. Sel. Areas Commun.*, vol. 37, no. 1, pp. 216–232, Jan. 2019.

[32] J. Liu, K. Xiong, Y. Lu, D. W. K. Ng, Z. Zhong, and Z. Han, "Energy efficiency in secure IRS-aided SWIPT," *IEEE Wireless Commun. Lett.*, vol. 9, no. 11, pp. 1884–1888, Nov. 2020.

[33] Z. Chu, Z. Zhu, F. Zhou, M. Zhang, and N. Al-Dhahir, "Intelligent reflecting surface assisted wireless powered sensor networks for Internet of Things," *IEEE Trans. Commun.*, vol. 69, no. 7, pp. 4877–4889, Jul. 2021.

[34] S. Zargari, A. Khalili, Q. Wu, M. R. Mili, and D. W. K. Ng, "Max–Min fair energy-efficient beamforming design for intelligent reflecting surface-aided SWIPT systems with non-linear energy harvesting model," *IEEE Trans. Veh. Technol.*, vol. 70, no. 6, pp. 5848–5864, Jun. 2021.

[35] Z. Chu, Z. Zhu, X. Li, F. Zhou, L. Zhen, and N. Al-Dhahir, "Resource allocation for IRS-assisted wireless-powered FDMA IoT networks," *IEEE Internet Things J.*, vol. 9, no. 11, pp. 8774–8785, Jun. 2022.

[36] S. Kim, H. Lee, J. Cha, S.-J. Kim, J. Park, and J. Choi, "Practical channel estimation and phase shift design for intelligent reflecting surface empowered MIMO systems," *IEEE Trans. Wireless Commun.*, vol. 21, no. 8, pp. 6226–6241, Aug. 2022.

[37] Z. Ding and H. V. Poor, "A simple design of IRS-NOMA transmission," *IEEE Commun. Lett.*, vol. 24, no. 5, pp. 1119–1123, Feb. 2020.

[38] Z. Ding, R. Schober, and H. V. Poor, "On the impact of phase shifting designs on IRS-NOMA," *IEEE Wireless Commun. Lett.*, vol. 9, no. 10, pp. 1596–1600, Oct. 2020.

[39] Z.-Q. He and X. Yuan, "Cascaded channel estimation for large intelligent metasurface assisted massive MIMO," *IEEE Wireless Commun. Lett.*, vol. 9, no. 2, pp. 210–214, Feb. 2020.

[40] Z. Wang, L. Liu, and S. Cui, "Channel estimation for intelligent reflecting surface assisted multiuser communications: Framework, algorithms, and analysis," *IEEE Trans. Wireless Commun.*, vol. 19, no. 10, pp. 6607–6620, Oct. 2020.

[41] A. Taha, M. Alrabeiah, and A. Alkhateeb, "Enabling large intelligent surfaces with compressive sensing and deep learning," *IEEE Access*, vol. 9, pp. 44304–44321, 2021.

[42] J. Chen, Y.-C. Liang, H. V. Cheng, and W. Yu, "Channel estimation for reconfigurable intelligent surface aided multi-user mmWave MIMO systems," *IEEE Trans. Wireless Commun.*, vol. 22, no. 10, pp. 6853–6869, Oct. 2022.

[43] W. Wang, W. Ni, H. Tian, Z. Yang, C. Huang, and K.-K. Wong, "Safeguarding NOMA networks via reconfigurable dual-functional surface under imperfect CSI," *IEEE J. Sel. Topics Signal Process.*, vol. 16, no. 5, pp. 950–966, Aug. 2022.

[44] Y. Xu, G. Li, Y. Yang, M. Liu, and G. Gui, "Robust resource allocation and power splitting in SWIPT enabled heterogeneous networks: A robust minimax approach," *IEEE Internet Things J.*, vol. 6, no. 6, pp. 10799–10811, Dec. 2019.

[45] J. Hu, M. Li, K. Yang, S. X. Ng, and K.-K. Wong, "Unary coding controlled simultaneous wireless information and power transfer," *IEEE Trans. Wireless Commun.*, vol. 19, no. 1, pp. 637–649, Jan. 2020.

[46] L. Liu, R. Zhang, and K.-C. Chua, "Wireless information and power transfer: A dynamic power splitting approach," *IEEE Trans. Commun.*, vol. 61, no. 9, pp. 3990–4001, Sep. 2013.

[47] A. A. Nasir, X. Zhou, S. Durrani, and R. A. Kennedy, "Wireless-powered relays in cooperative communications: Time-switching relaying protocols and throughput analysis," *IEEE Trans. Commun.*, vol. 63, no. 5, pp. 1607–1622, May 2015.

[48] K. Xiong, B. Wang, and K. J. R. Liu, "Rate-energy region of SWIPT for MIMO broadcasting under nonlinear energy harvesting model," *IEEE Trans. Wireless Commun.*, vol. 16, no. 8, pp. 5147–5161, Aug. 2017.

[49] D. Xu, X. Yu, V. Jamali, D. W. K. Ng, and R. Schober, "Resource allocation for large IRS-assisted SWIPT systems with non-linear energy harvesting model," in *Proc. IEEE Wireless Commun. Netw. Conf. (WCNC)*, 2021, pp. 1–7.

[50] M. Bengtsson and B. Ottersten, "Optimum and suboptimum transmit beamforming," in *Handbook of Antennas in Wireless Communications*. Hoboken, NJ, USA: CRC Press, 2018, p. 18.

[51] I. Ahmed et al., "A survey on hybrid beamforming techniques in 5G: Architecture and system model perspectives," *IEEE Commun. Surveys Tuts.*, vol. 20, no. 4, pp. 3060–3097, 4th Quart., 2018.

[52] J. Zhu, J. Wang, Y. Huang, K. Navaie, Z. Ding, and L. Yang, "On optimal beamforming design for downlink MISO NOMA systems," *IEEE Trans. Veh. Technol.*, vol. 69, no. 3, pp. 3008–3020, Jan. 2020.

[53] T. Wang, F. Fang, and Z. Ding, "An SCA and relaxation based energy efficiency optimization for multi-user RIS-assisted NOMA networks," *IEEE Trans. Veh. Technol.*, vol. 71, no. 6, pp. 6843–6847, Mar. 2022.

[54] Z.-Q. Luo, W.-K. Ma, A. M.-C. So, Y. Ye, and S. Zhang, "Semidefinite relaxation of quadratic optimization problems," *IEEE Signal Process. Mag.*, vol. 27, no. 3, pp. 20–34, May 2010.

[55] M. F. Anjos and J. B. Lasserre, *Handbook on Semidefinite, Conic and Polynomial Optimization*, vol. 166. New York, NY, USA: Springer, 2011.

[56] M. Schubert and H. Boche, "Solution of the multiuser downlink beamforming problem with individual SINR constraints," *IEEE Trans. Veh. Technol.*, vol. 53, no. 1, pp. 18–28, Jan. 2004.

[57] Y. Huang and D. P. Palomar, "Rank-constrained separable semidefinite programming with applications to optimal beamforming," *IEEE Trans. Signal Process.*, vol. 58, no. 2, pp. 664–678, Feb. 2010.

[58] E. Björnson and E. Jorswieck, *Optimal Resource Allocation in Coordinated Multi-cell Systems*. London, U.K.: Now, 2013.

[59] H. Dahrouj and W. Yu, "Coordinated beamforming for the multicell multi-antenna wireless system," *IEEE Trans. Wireless Commun.*, vol. 9, no. 5, pp. 1748–1759, May 2010.

[60] W. Yu and T. Lan, "Transmitter optimization for the multi-antenna downlink with per-antenna power constraints," *IEEE Trans. Signal Process.*, vol. 55, no. 6, pp. 2646–2660, Jun. 2007.

[61] A. B. Gershman, N. D. Sidiropoulos, S. Shahbazpanahi, M. Bengtsson, and B. Ottersten, "Convex optimization-based beamforming," *IEEE Signal Process. Mag.*, vol. 27, no. 3, pp. 62–75, May 2010.

[62] E. Björnson, M. Bengtsson, and B. Ottersten, "Optimal multiuser transmit beamforming: A difficult problem with a simple solution structure [lecture notes]," *IEEE Signal Process. Mag.*, vol. 31, no. 4, pp. 142–148, Jul. 2014.

[63] A. Wiesel, Y. C. Eldar, and S. Shamai, "Zero-forcing precoding and generalized inverses," *IEEE Trans. Signal Process.*, vol. 56, no. 9, pp. 4409–4418, Sep. 2008.

[64] M. Joham, W. Utschick, and J. Nossek, "Linear transmit processing in MIMO communications systems," *IEEE Trans. Signal Process.*, vol. 53, no. 8, pp. 2700–2712, Aug. 2005.

[65] E. Biglieri, R. Calderbank, A. Constantinides, A. Goldsmith, A. Paulraj, and H. V. Poor, *MIMO Wireless Communications*. Cambridge, U.K.: Cambridge Univ. Press, 2007.

[66] M. Grant and S. Boyd. "CVX: MATLAB software for disciplined convex programming, version 2.1." 2014. [Online]. Available: https://www.researchgate.net/publication/229058225_CVX_MATLAB _software_for_disciplined_convex_programming

[67] M. Hua, Q. Wu, D. W. K. Ng, J. Zhao, and L. Yang, "Intelligent reflecting surface-aided joint processing coordinated multipoint transmission," *IEEE Trans. Commun.*, vol. 69, no. 3, pp. 1650–1665, Mar. 2021.

AHMAD KAMAL HASSAN received the B.Eng. degree (Hons.) in electrical and electronics engineering from the University of Bradford in 2007, the M.S. degree in electrical engineering from Karlstad University in 2012, and the Ph.D. degree in electrical and computer engineering from King Abdulaziz University in 2017. From 2007 to 2010, he served as a Consultant with Nokia Siemens Networks, Ericsson AB, and Advance Communication and Electronics Systems. He was a Research Associate with the Ghulam Ishaq Khan Institute of Engineering Sciences and Technology from 2013 to 2014, where he has been an Assistant Professor since 2017 and an Associate Professor since 2023. His research interests include system modeling and performance analysis of emerging communication systems. He is a Chartered Engineer and a member of the Institution of Engineering and Technology.

ZIAUL HAQ ABBAS received the M.Phil. degree in electronics from Quaid-e-Azam University, Pakistan, in 2001, and the Ph.D. degree from the Agder Mobility Laboratory, Department of Information and Communication Technology, University of Agder, Norway, in 2012. In 2012, he was a Visiting Researcher with the Department of Electrical and Computer Engineering, University of Minnesota, USA. He is currently a Professor with the Faculty of Electrical Engineering and a Co-Founding Member of the Telecommunications and Networking Research Laboratory, Ghulam Ishaq Khan Institute of Engineering Sciences and Technology. His research interests include energy efficiency in hybrid mobile and wireless communications networks, 4G and beyond mobile systems, mesh and ad hoc networks, traffic engineering in wireless networks, performance evaluation of communications protocols and networks by analysis and simulation, quality-of-service in wireless networks, green wireless communications, and cognitive radio.

HALEEMA SADIA received the B.Sc. degree in telecommunication engineering from the University of Engineering and Technology, Taxila, Pakistan, in 2015, the M.S. degree in electrical engineering from the College of Electrical and Mechanical Engineering NUST, Pakistan, in 2018, and the Ph.D. degree in electrical engineering from the Ghulam Ishaq Khan (GIK) Institute of Engineering Sciences and Technology, Pakistan, in 2024, where she was a Graduate Research Assistant from 2021 to 2024. She worked as a Research Assistant with HITEC University Taxila, Pakistan, from 2015 to 2016. She also served as an IT Instructor with USF from 2018 to 2021. She is currently a Postdoctoral Research Fellow with the Department of Electrical and Communication Engineering, College of Engineering, United Arab Emirates University, Al Ain, UAE. Her research areas include wireless communication networks, NOMA for 5G networks, multiuser MIMO systems, intelligent reflecting surfaces, optimization techniques for B5G networks, and ML for 5G and B5G wireless networks.

GHULAM ABBAS (Senior Member, IEEE) received the B.S. degree in computer science from the University of Peshawar, Pakistan, in 2003, and the M.S. degree in distributed systems and the Ph.D. degree in computer networks from the University of Liverpool, U.K., in 2005 and 2010, respectively. From 2006 to 2010, he was Research Associate with Liverpool Hope University, U.K., where he was associated with the Intelligent and Distributed Systems Laboratory. Since 2011, he has been with the Faculty of Computer Sciences and Engineering, Ghulam Ishaq Khan (GIK) Institute of Engineering Sciences and Technology, Pakistan. He is currently working as a Professor and the Director of Huawei Network Academy. He is a Co-Founding Member of the Telecommunications and Networking Research Laboratory, GIK Institute of Engineering Sciences and Technology. His research interests include computer networks and wireless and mobile communications. He is a Fellow of the Institute of Science and Technology, U.K., and the British Computer Society.

THAR BAKER (Senior Member, IEEE) is currently a Professor of Industry 4.0/5.0 with the School of Architecture, Technology and Engineering, University of Brighton, Brighton, U.K. He was a Reader of Cloud Engineering and the Head of the Applied Computing Research Group, Faculty of Engineering and Technology, Liverpool John Moores University, Liverpool, U.K. He spent a few years with the College of Computing and Informatics, University of Sharjah, Sharjah, UAE. His research interests include cloud and grid computing, edge AI, Internet of Things, sensor networks, and federated learning. He is a Senior Fellow of HEA.

NASIR SAEED (Senior Member, IEEE) received the B.Sc. degree in telecommunication from the University of Engineering and Technology, Peshawar, Pakistan, in 2009, the M.Sc. degree in Satellite Navigation from the Polito di Torino, Italy, in 2012, and the Ph.D. degree in electronics and communication engineering from Hanyang University, Seoul, South Korea, in 2015. He was an Assistant Professor with the Department of Electrical Engineering, IQRA National University, Peshawar, from 2015 to 2017. From July 2017 to December 2020, he was a Postdoctoral Research Fellow with the Communication Theory Laboratory, King Abdullah University of Science and Technology, Saudi Arabia. He is currently an Associate Professor with the Department of Electrical and Communication Engineering, United Arab Emirates University, Al Ain, UAE. He has published more than 80 international journal and conference articles. His research interests include non-conventional communication networks, heterogeneous vertical networks, multidimensional signal processing, and localization. He is also an Associate Editor of IEEE WIRELESS COMMUNICATIONS LETTERS.